Geol. Mag. **142** (5), *2005, pp. 583–604.* © *2005 Cambridge University Press*
doi:10.1017/S0016756805000890 *Printed in the United Kingdom*

Geomorphic evolution of a storm-dominated carbonate ramp (*c*. 549 Ma), Nama Group, Namibia

S. DIBENEDETTO & J. GROTZINGER*

Department of Earth, Atmospheric and Planetary Sciences, Massachusetts Institute of Technology, Cambridge, MA 02139, USA

(*Received* 25 April 2004; *accepted* 5 April 2005)

Abstract – The well-exposed Hoogland Member (*c*. 549 Ma) of the northern Nama Group (Kuibis Subgroup), Namibia, represents a storm-dominated carbonate ramp developed in a foreland basin of terminal Proterozoic age. The ramp displays facies gradients involving updip grainstones which pass downdip into broad, spatially extensive tracts of microbial laminites and finely laminated mudstones deposited above and below storm wave base. Trough cross-bedded, coarse grainstones are shown to transit downdip into finer-grained calcarenites, irregular microbial laminites and mottled laminites. Siliciclastic siltstones and shales were deposited further downdip. Platform growth was terminated through smothering by orogen-derived siliciclastic deposits. Ramp morphology was controlled by several different processes which acted across many orders of magnitude (millimetres to kilometres), including *in situ* growth of mats and reefs, scouring by wave-produced currents, and transport and infilling of coarse-grained carbonates and fine-grained carbonates and clastics. At the smallest scale, 'roughening' of the sea-floor through heterogeneous trapping and binding by microbial mats was balanced by smoothing of the sea-floor through accumulation of loose sediment to fill the topographic lows within the upward-propagating mat. At the next scale up, parasequence development involved roughening of the sea-floor through shoal growth and grainstone progradation, balanced by sea-floor smoothing through shale infilling of resulting downdip accommodation, as well as the metre-scale topographic depressions within the mosaic of shoal-water facies. At even larger (sequence/platform) scales, roughening of the sea-floor occurred through aggradation and progradation of thick carbonates, balanced by infilling of the foreland basin with orogen-derived siliciclastic sediments. At all scales a net balance was achieved between sea-floor roughening and sea-floor smoothing to maintain a more or less constant ramp profile.

Keywords: carbonate, geomorphology, platform, ramp, Proterozoic.

1. Introduction

Evaluation of the mechanisms by which geomorphic variability is propagated across spatial and temporal scales has become a growing focus of research in the earth sciences (Howard, 1997; Paola *et al*. 2001; Dietrich *et al*. 2003) with potential application to carbonate depositional systems (Drummond & Dugan, 1999; Burgess, 2001; Burgess, Wright, & Emery, 2001; Rankey, 2002; Burgess & Wright, 2003). Pattern formation in these systems at scale 'n' characteristically results from interactions between intrinsic component subsystems at scale 'n − 1' (self organization), perhaps modulated by processes at scale 'n + 1' (extrinsic forcing). Sedimentary geologists have historically recognized the impacts of these 'autocyclic' and 'allocyclic' processes on stratigraphic stacking patterns; recent models which simulate these interactions generate significant complexity in stratal stacking patterns (Burgess & Wright, 2003) and provide realistic facies distributions similar to certain ancient platforms. These studies highlight the need for further field studies to characterize the portions of carbonate platforms which express development across a number of scales, with emphasis on defining the breaks in scales where changes in processes may occur. A key question involves untangling the relationship between these processes to control the geomorphic evolution of the platform, which is only partially preserved in the record of facies distributions and stratal patterns.

The Hoogland platform, Nama Group, Namibia (Fig. 1) formed as a storm-dominated carbonate ramp and provides a case study of the geomorphic evolution of carbonate platform across a variety of spatial and temporal scales. The terminal Proterozoic age (*c*. 549 Ma) of this ramp insures that important records of sediment transport, deposition and erosion processes have not been erased through the destructive effects of burrowing, a concern raised by Burgess & Wright (2003). Excellent exposures of the undeformed platform throughout a dendritic canyon system provide the opportunity for a high-resolution architectural study, at a variety of scales, of the short- to long-term morphological evolution of this ramp (Fig. 2).

* Author for correspondence: grotz@mit.edu

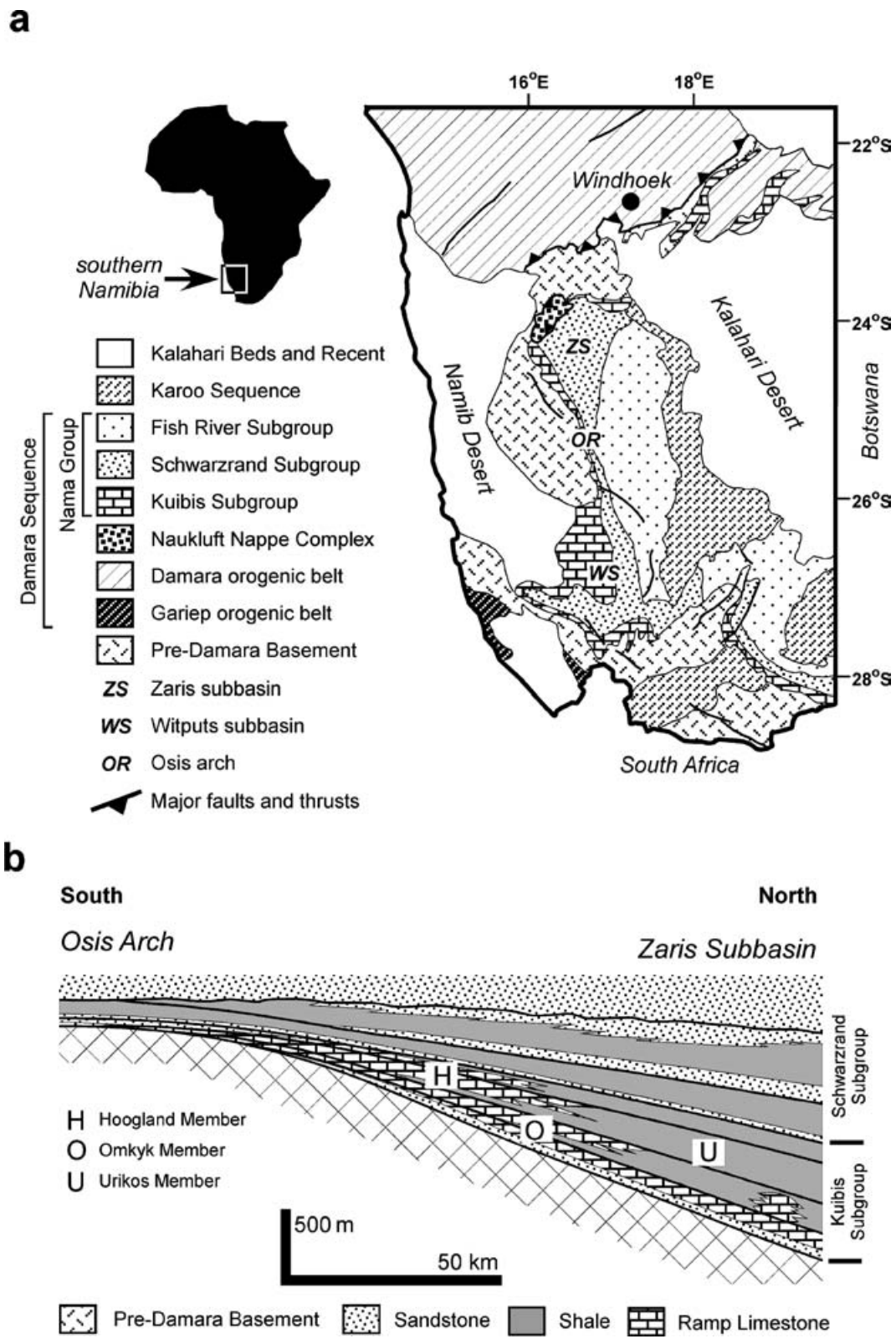

Figure 1. (a) Generalized geological map of Southern Namibia showing eastward younging of Nama Group exposures. Zaris and Witputs refer to subbasins of the Nama foreland basin separated by the Osis Arch structural high. (b) Regional stratigraphy of Zaris subbasin north of Osis Arch (modified from Germs, 1983). The basal Kuibis carbonate platform interfingers with the Urikos Member and was buried by the shallow marine siliciclastics of the Schwarzrand Subgroup and molasse deposits of the Fish River Subgroup. The Hoogland Member is the focus of this study.

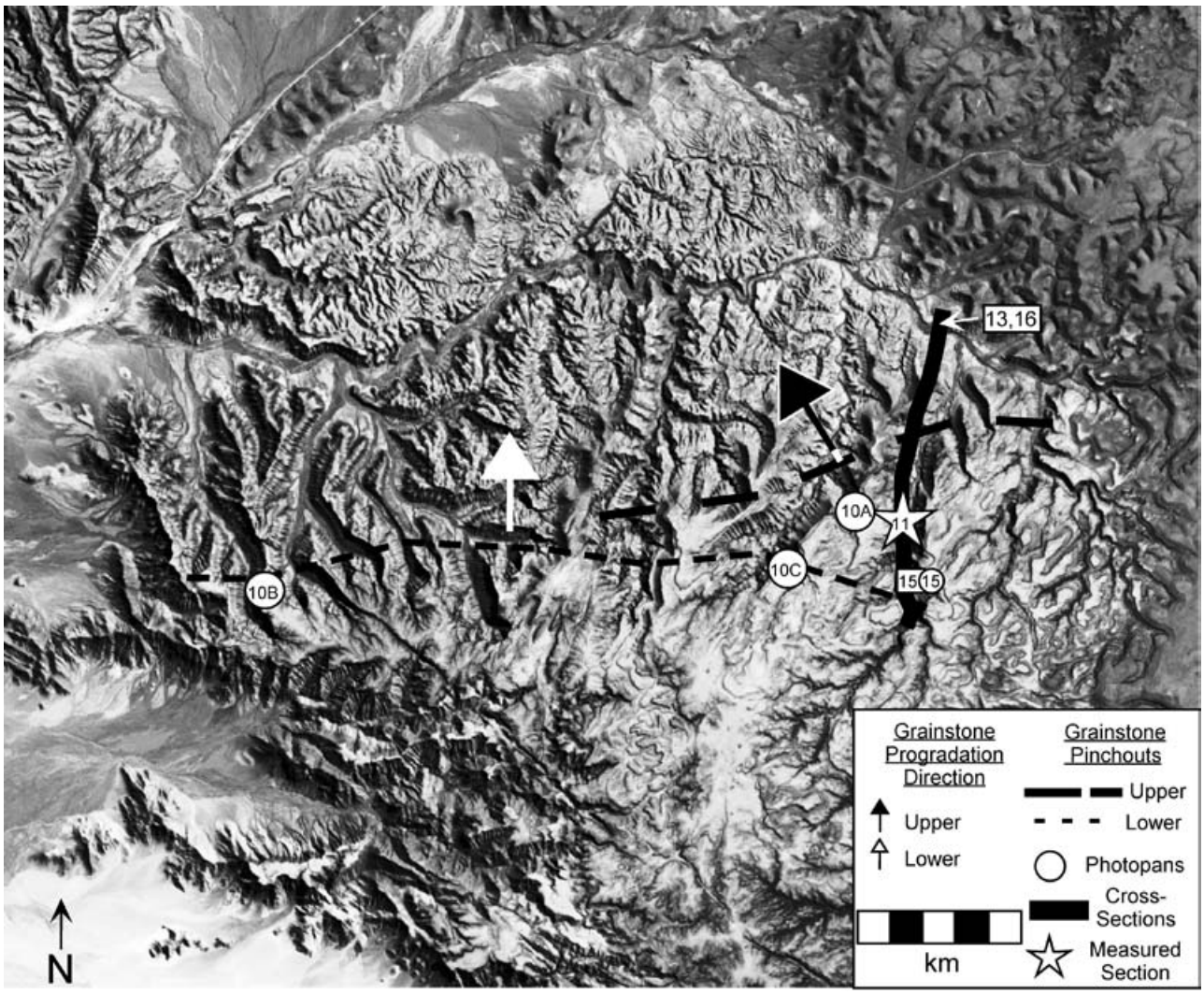

Figure 2. LANDSAT TM Image of study area showing positions of reference section (Fig. 9), bed tracing, and photograph locations (Figs 10a, 10c, 11, 13, 15, 16). Grey-scale image reveals regional geology; medium grey to white areas in centre are limestones and dolostones of Kuibis Subgroup, light grey-white area to the southeast is shales of the Urikos Member, and dark grey area to the north and east is siliciclastics of Schwarzrand Subgroup. Note extensive canyon incision providing the opportunity for section correlation in three dimensions. Location of grainstone pinchouts determined by linear projection between pinchout points in laterally adjacent canyons (see text).

2. Geological setting

The Nama Group fills a foreland basin related to convergence and overthrusting in the flanking Damara Orogen (Germs, 1983). In the northern part of the Nama basin (Zaris subbasin), the Kuibis Subgroup represents a northward-tapering carbonate ramp that thins southward towards the Osis Arch, the forebulge of the basin (Fig. 1; Germs, 1983). A regionally correlative ash bed within the middle Kuibis (basal Hoogland Member) provides a U–Pb zircon age of 548.8 ± 1 Ma (Grotzinger *et al*. 1995). Shallow marine siliciclastic sediments of the Schwarzrand Subgroup interfinger with and overlie the carbonates of the Kuibis Subgroup and are overlain by the shallow marine to fluvial Fish River Subgroup (Fig. 1).

The Kuibis Subgroup comprises two formations: the basal Dabis Formation, a transgressive sheet sandstone generally only a few metres thick, and the overlying Zaris Formation, which consists of shallow marine carbonates and shales up to several hundred metres thick. The Zaris is composed of a lower Omkyk Member and overlying Hoogland Member, which together define a backward-stepping (cratonward) sequence set of carbonate ramp deposits. The Urikos Member is a thick shale deposit which interfingers with carbonates in downdip positions, and overlies them in updip positions.

The basal Omkyk Member forms a ramp succession which extends in excess of 150 km downdip, and is composed of trough cross-bedded and hummocky cross-stratified grainstones that contain numerous thrombolite–stromatolite reef horizons, carbonate

mudstones and shales (O. Smith, unpub. M.Sc. thesis, Massachusetts Inst. Tech., 1999; Grotzinger, 2000). The overlying Hoogland Member forms a ramp that contains a smaller but coarser volume of grainstone, contains more shale, lacks significant reefs, and has a dip extent of less than 100 km (S. DiBenedetto, unpub. M.Sc. thesis, Massachusetts Inst.Tech., 2002). The Hoogland Member is the focus of the present study and marks the final episode of significant carbonate deposition within the northern Nama basin. Growth was terminated due to high influx of orogen-derived clastics.

3. Facies descriptions

Lithofacies are presented in Table 1 and described briefly below. Facies are presented according to their palaeogeographic position, starting with updip inner-ramp coarse grainstones and continuing downdip through the distal mid-ramp mottled laminites (Fig. 3). The current study area does not expose the most updip (shoreline) or the most downdip (basinal) facies.

3.a. Coarse grainstone

Coarse grainstones (Fig. 4a–c) form two prominent lithostratigraphic units (Lower and Upper Grainstone units) and display trough and tabular cross-bedding. Hummocky cross-stratification substitutes for cross-bedding at the downdip limits of grainstone bodies. Grain types consist principally of coated intraclasts and ooids; a cut-off size of 1 mm distinguishes these grainstones from the finer calcarenite facies.

3.b. Calcarenite

Calcarenites are formed of fine to coarse grains, although determination of grain types is difficult due to pervasive recrystallization. Bedding is characterized by planar lamination, quasi-planar lamination, hummocky cross-stratification, wavy-bedding, and ripple and trough cross-bedding (Fig. 4d). Hummocks have wavelengths of up to several metres which indicate deposition in inner-ramp to proximal outer-ramp settings, within storm wave base (Arnott, 1993; Siringan & Anderson, 1994).

3.c. Irregular and mottled laminites

Irregular laminites are widespread in relatively updip, inner- to mid-ramp positions (Fig. 3) and consist of sub-millimetre microbial laminae typically expressed by an undulatory lamination style (Fig. 4e). The lack of finer-grained sediments, and the presence of coarse grainstone-filled scours within the irregular laminites, indicates that these updip mats were under the influence of regularly moving water currents. In more proximal, updip positions, stromatolites are present (Fig. 4f) and laminae often are scoured. The irregular laminites are

Table 1. Summary of facies in the Hoogland Member, and their attributes

Facies	Stratigraphic position	Bedding attributes	Sedimentary structures	Grain size	Depositional environment
Coarse grainstone	Lower and upper grainstone units	Massive to thick bedded; forms clinoform tongues	HCS, trough cross-bedding	Rudite to coarse grained	Wave-swept inner-ramp within fair-weather wave base
Calcarenite	All units; most abundant in updip Gametrail unit	Thick to thin beds interbedded with irregular laminite and intraclast conglomerate	HCS, climbing ripples, planar and quasiplanar lamination	Fine to coarse grained	Inner- to outer-ramp; within fair-weather to storm wave base
Intraclast conglomerate	All units; commonly towards tops of parasequences	Thick to thin beds of random to horizontally imbricated clasts	Some lenses of edgewise conglomerate	Platy rudite	Ripped up transported and deposited during individual storm events
Irregular laminite	Gametrail and breccia units	Undulatory; smooth topped, thick to thin laminations of alternating light/dark calcisiltite/lutite	Stromatolites form updip; truncated laminae	Silt to mud	Distal inner- to distal mid-ramp positions within lower fair-weather wave base
Mottled laminite	Heterolithic unit	Rough-topped, smooth-bottomed, thickly-laminated alternating light/dark calcisiltite/lutite layers	Increasingly stylolitized downdip	Silt to mud	Mid- to outer-ramp within storm wave base
Matrix-supported breccia	Breccia unit	Massive disruption of up to 7 m of previously deposited stratigraphy; trace downdip into fining upwards, intraclastic tempestites	Graded bedding; incipient brecciation; large blocks	Silt to mud matrix of sheared irregular laminite; slabs and rafts up to 1.5 m × 5 m	Updip storm triggered; perhaps slope/gravitationally enhanced
Shale	Heterolithic and breccia units, at bases of parasequences	Massive; sometimes thinly interlaminated with lime mudstones	Rare flaser bedding; fine lamination	Silt to mud	Outer-ramp clastics shed from side of basin opposite to carbonate platform

HCS–hummocky cross-stratified.

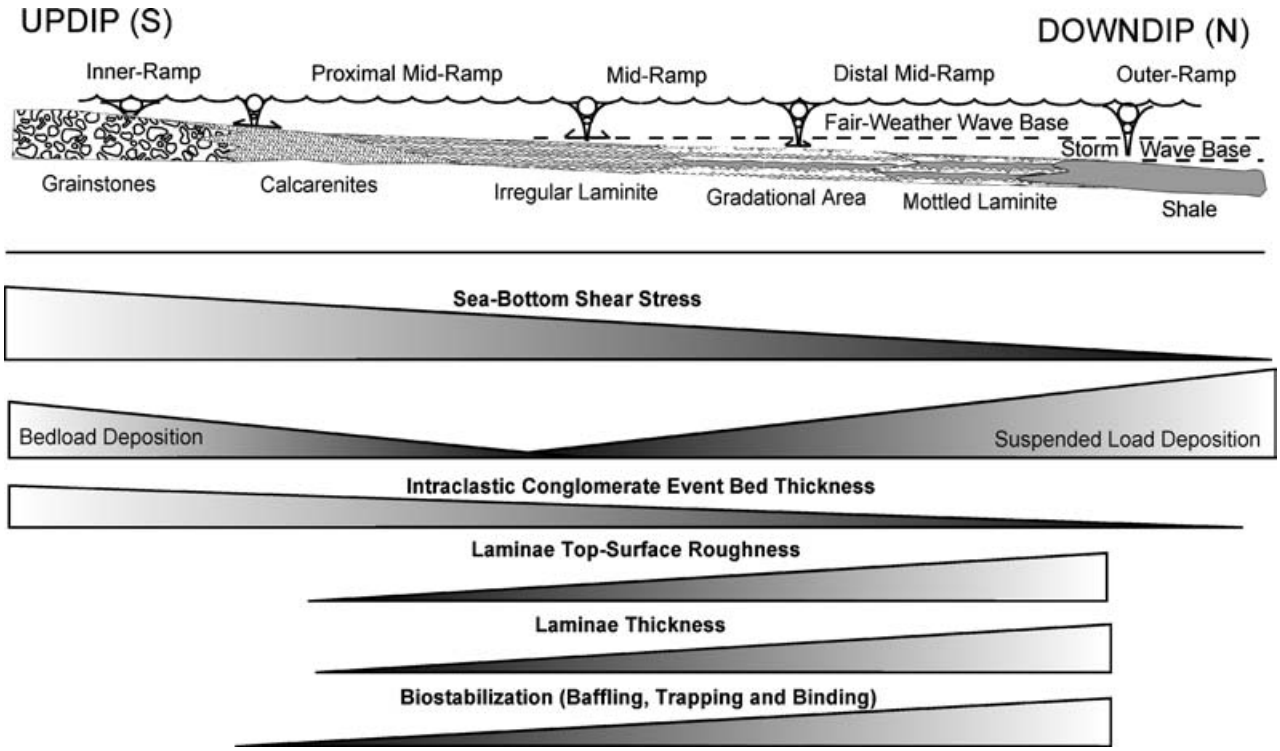

Figure 3. Hoogland ramp facies model illustrating the relative palaeogeographic position, palaeoenvironmental interpretations, and general bedding/lamination trends observed along chronostratigraphic horizons. Updip coarse grainstones and calcarenites are found to transit downdip into finer-grained, microbial, irregular and mottled laminites and shales. Double headed arrows at bases of schematic wave orbits represent relative oscillatory shear stresses along platform sea-bottom. Note the relationship between laterally adjacent facies belts and their vertical stacking patterns to form parasequences throughout the Hoogland Member.

interpreted to be one of the primary fixers as well as sources of carbonate grains on the Hoogland ramp. Fixing resulted from the processes of trapping and binding of traction-transported sediments, and early cementation. As a sediment source, production of coarse, platy intraclasts and finer granular sediments occurred through the erosion of these sediments. During their formation, therefore, it seems likely that these facies record significant non-deposition, bypassing, and even erosion.

The mottled laminite facies is characterized by the alternation of dark laminae of microbial origin, and light laminae representing fine carbonate mud and silt (Fig. 5). The characteristic mottled texture is created by outward-radiating, spherulitic arrangements of matrix-replacive neomorphic calcite that nucleated and accreted away from a point (Fig. 5b, c). Bed tracing of chronostratigraphically bounded horizons reveals that this facies is found downdip of the irregular laminites. The mottled laminites formed by benthic trapping and binding of finer carbonates which accumulated through fallout from suspension. The lower energy, distal, mid- to outer-ramp setting of the mottled laminites is indicated by a general lack of wave-produced sedimentary structures and fine- to coarse-grained carbonate sediment emplaced by traction currents.

The involvement of benthic microbial communities in formation of the irregular and mottled laminite facies is indicated by the presence of fine lamination, the irregular to wavy geometry of laminae, the occurrence of locally truncated laminae and the local growth of stromatolites with synoptic relief (e.g. Burne & Moore, 1987; Chafetz & Buczynski, 1992). Both laminite types are characterized by couplets of darker laminae with rough lamina tops that alternate with lighter laminae with smooth lamina tops. The rough-topped dark laminae, inferred to have formed in the presence of microbial mats, create rough micro-topography along their top surface. Superjacent light laminae, inferred to have been sediment-rich, smooth over this micro-topography produced by the mats (or mat-induced processes), and thus prevent it from being inherited and amplified in subsequent events of sedimentation during microbial mat growth (Fig. 6). Once deposited, gravitational forces and traction currents moved these sediments from the tops and flanks of micro-topographic features into adjacent lows and thus smoothed relief.

3.d. Intraclastic conglomerate

These clast-supported, platy, intraclast grainstones and packstones occur as sheet-like beds or as isolated lenses with flat bases and mounded tops, showing polygonal packing of clasts (Fig. 7b, c). These features indicate deposition under oscillatory flow conditions,

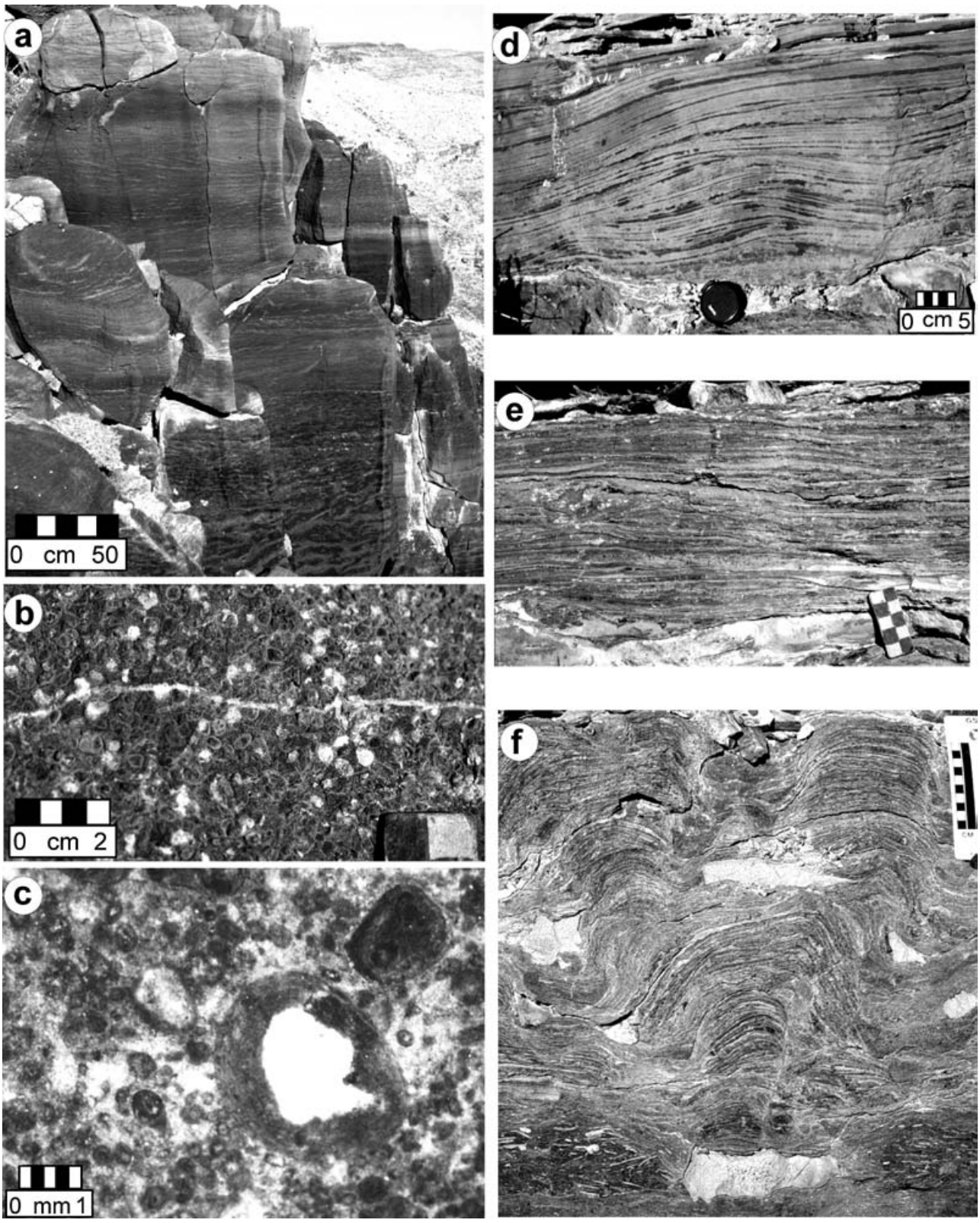

Figure 4. Coarse grainstone facies. (a) Tabular cross-bed sets within the updip Lower Grainstone unit. (b) Outcrop photograph showing replaced rims; dark intergrain areas are marine cement. Light areas are sparry void-filling cements and fracture fill. (c) Microphotograph of leached cortex. Note oolitic rims, poorly sorted grains and abundance of light-coloured, sparry, void-filling cement. (d) Hummocky cross-stratification in calcarenite facies. Note low-angle truncations that pass laterally into concordant surfaces. This facies is found in mid-ramp positions usually interbedded with irregular laminites and indicates storm deposition under long-period combined flow conditions with high sediment concentrations. (e) Mid-ramp irregular laminite. Note relatively continuous and alternating dark (microbial) and light (sediment-rich) laminae. (f) Stromatolites in updip irregular laminites. Note similarity in lamination texture to (a); nucleation of growth on clast of lime mudstone within the intraclastic conglomerate base; branching above elongate calcisiltite clast at top centre; and light coloured pockets of calcisiltite present at sharp bends in stromatolite.

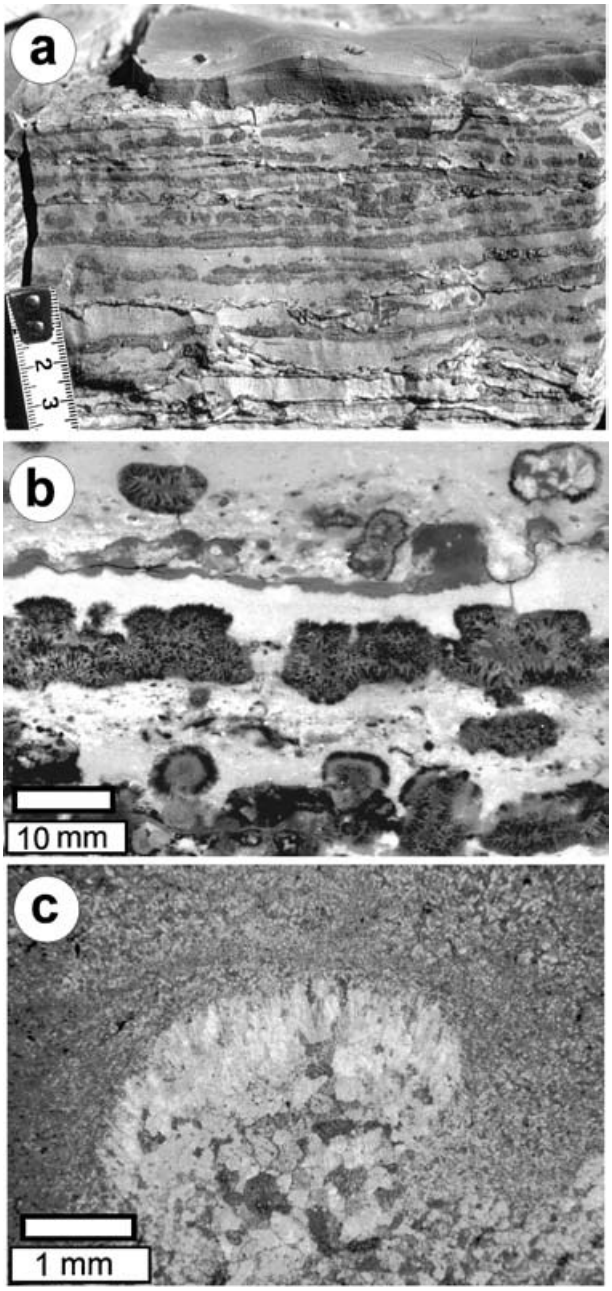

Figure 5. Mottled laminite facies. (a) Outcrop photo illustrates how light-coloured calcisiltite laminae damp out micro-topography at the tops of darker microbial laminae. Scale in cm. (b) Scanned polished slab showing internal crystal textures to mottles. Note internal dog-tooth spar, which contrasts with dark-coloured, outward-radiating fringes on some mottles. Also note how relief along rough-topped mottles at centre is damped and reset to flat surface by deposition and infilling of overlying light calcisiltite laminae. (c) Photomicrograph of mottle showing compaction of calcilutite grains over radiating fan of acicular calcite, which is interpreted to have grown as a small-scale crystal fan at the sediment–water interface.

preserving the deceleration and changing of direction of the wave orbit (Mount & Kidder, 1993). Clasts within both types of conglomerate are composed of early-cemented fragments of the irregular laminite facies. Individual intraclastic event beds are interpreted as

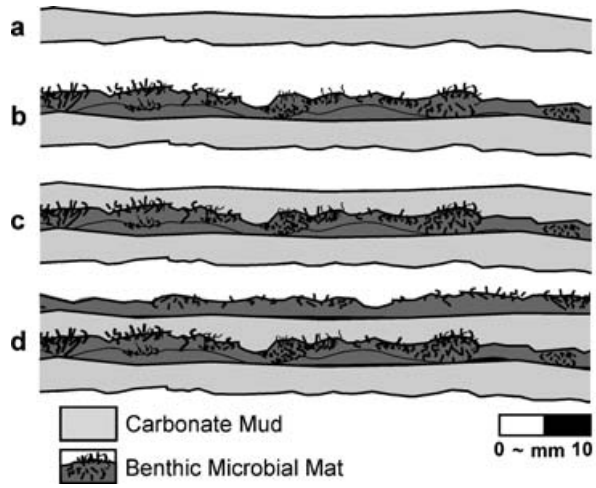

Figure 6. Bed-scale processes affecting sea-bottom morphology. (a) Relatively smooth-topped calcisiltite laminae, which smothered and damped pre-existing micro-topography of underlying microbial lamina, serve as nucleation surface for microbial mat. (b) Upward growth and accretion of benthic microbial mat creating rough top-surface relief of darker laminae. (c) Event-related (e.g. whiting, or storm) deposition of fine- to mud-sized lighter-coloured carbonate sediment that covers and fills in the nooks and crannies of the microbial mat leaving a smooth lamina top. (d) Recolonization and growth of the mat to produce another darker, rougher lamina.

tempestites, triggered by storms and associated high energy conditions (Aigner, 1982; Mount & Kidder, 1993). However, in contrast to their hummocky siliciclastic counterparts, the bases of these carbonate beds are rarely found to be significantly erosional, which most likely reflects early cementation of the sea-floor.

3.e. Matrix supported breccias

Breccias consist of platy intraclasts of microbial laminites supported by a fine-grained carbonate matrix (Fig. 7d, e). The thicknesses of breccia beds range from less than 10 cm to greater than 700 cm. The breccias locally cut underlying strata for thicknesses of up to a few metres, but are otherwise concordant. In contrast, the upper contacts of breccia-containing units are everywhere concordant with overlying strata (Fig. 7e), often passing upward into planar-stratified to hummocky cross-stratified calcarenite beds. These calcarenites are formed through the progressive reduction in size of breccia clasts and their incorporation into the base of the storm bed (Fig. 7a).

The systematic relationship between the occurrence of storm deposits and breccias suggests that storms may have been responsible for breccia development. The process of cyclic wave loading invoked by Seguret *et al*. (2001) may be partly invoked to explain some of the features observed in the Hoogland breccias. Cyclic wave loading of the sea-floor entails the periodic displacement of sub-surface sediments (Suhayda, 1977), such that slowly applied shear stresses strain the strata and liquefy the muds as pore pressures

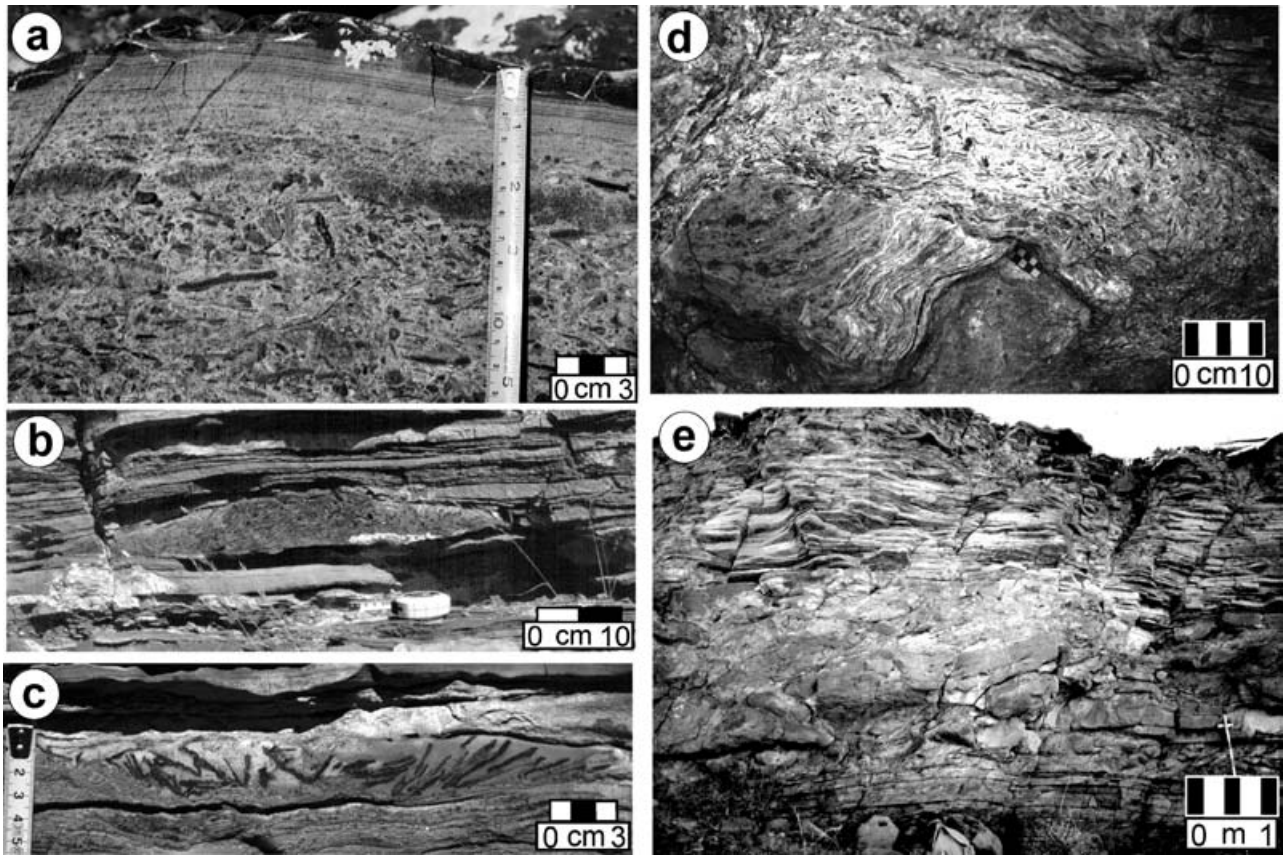

Figure 7. Intraclastic conglomerate and breccia facies. (a) Graded bedding and planar-laminated cap within a tempestite bed. (b) Lens of clast-supported edgewise intraclast conglomerate interbedded with calcisiltites and irregular laminites. The tapered edges and splayed clast packing patterns within this lens indicate that is was likely deposited by oscillatory flow. (c) Lens of matrix-supported edgewise conglomerate. Note radial packing of these irregular laminite intraclasts. (d) Partially deformed beds of irregular laminite sharply truncated by the matrix-supported breccia facies. (e) Larger-scale deformation associated with brecciation. Note continuous stratigraphy above and below metre-scale breccia deposit at centre.

progressively increase (Clukey *et al*. 1985). Once the layer-parallel shear stresses in the sediments crossed a critical threshold, the thinly laminated microbially produced strata began to liquefy and fail, breaking off and detaching the rafts of intact stratigraphy floating in the matrix. As the storm swell dissipated, the continued application of layer-parallel shear stresses macerated any stratigraphy not already cemented to form the platy, intraclastic matrix. The newly produced slurry of platy intraclasts and larger rafts would have locked into place once the layer-parallel shear stresses decreased below the Bingham threshold for deformation (Seguret *et al*. 2001). A further decrease in current velocities and shear stresses resulted in the deposition of hummocky cross-stratified beds, overlain by wave-oscillation ripples observed at the tops of brecciated intervals.

4. Lithostratigraphic subdivision of Hoogland Member

The stratigraphy of the Hoogland Member is subdivided into five units according to their dominant lithofacies assemblages. In ascending order these are the Heterolithic, Gametrail, Lower Grainstone, Breccia and Upper Grainstone units (Figs 8, 9).

4.a. Heterolithic unit

The recessive weathering Heterolithic unit (Fig. 10a, c) is 30–40 m thick and contains a diverse lithofacies assemblage of interlayered thin- to medium-bedded mottled laminites, shales, lime mudstones and rare calcarenites (Figs 9, 11). The lower part of the Heterolithic unit represents deposition within a transgressive systems tract (TST), which commenced at the sequence boundary located immediately below the uppermost reefs in the Omkyk Member (Fig. 8; O. Smith, unpub. M.Sc. thesis, Massachusetts Inst. Tech., 1999; Grotzinger, 2000). The maximum flooding interval is placed above the last occurrence of small-scale stromatolitic bioherms, approximately ten metres above the basal contact with the Omkyk Member. Bed tracing along a marker ash bed (548.8 Ma; Grotzinger *et al*. 1995) in the middle Heterolithic unit (Fig. 9) reveals that individual thin to medium beds of calcisiltite, shale and mottled laminite can be traced and correlated for

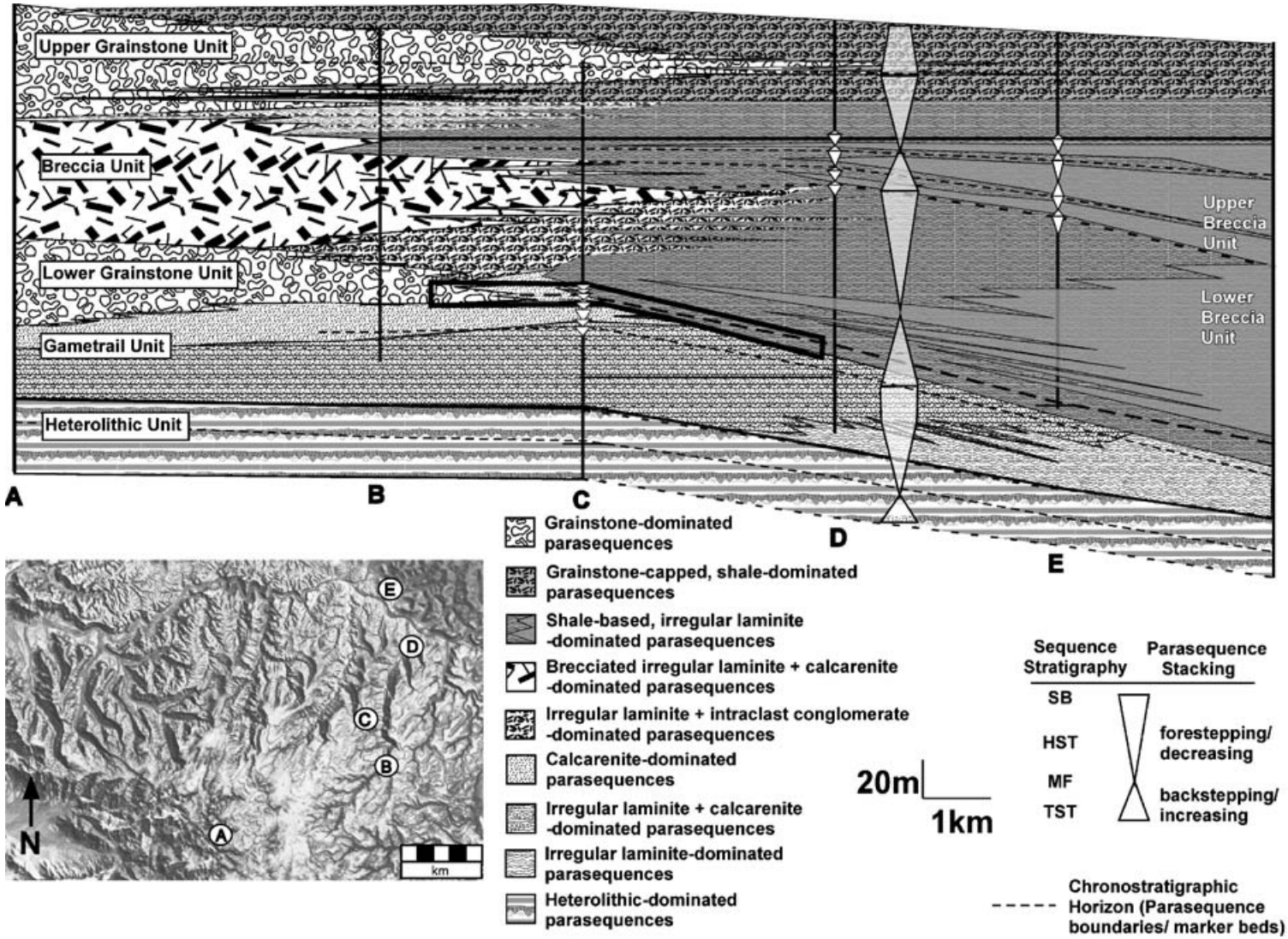

Figure 8. Regional cross-section of Hoogland Member showing generally coarser-grained, updip parasequences at left, passing downdip into deeper-water, finer-grained parasequences. Datum is top of regionally extensive parasequence in upper Breccia unit (see Figs 9, 15). Large triangles show interpreted long term (sequence-scale) changes in accommodation regime and sequence stratigraphy as determined from parasequence stacking patterns. Smaller triangles are individual parasequences. Box at centre is position of bed tracing shown in Figure 12.

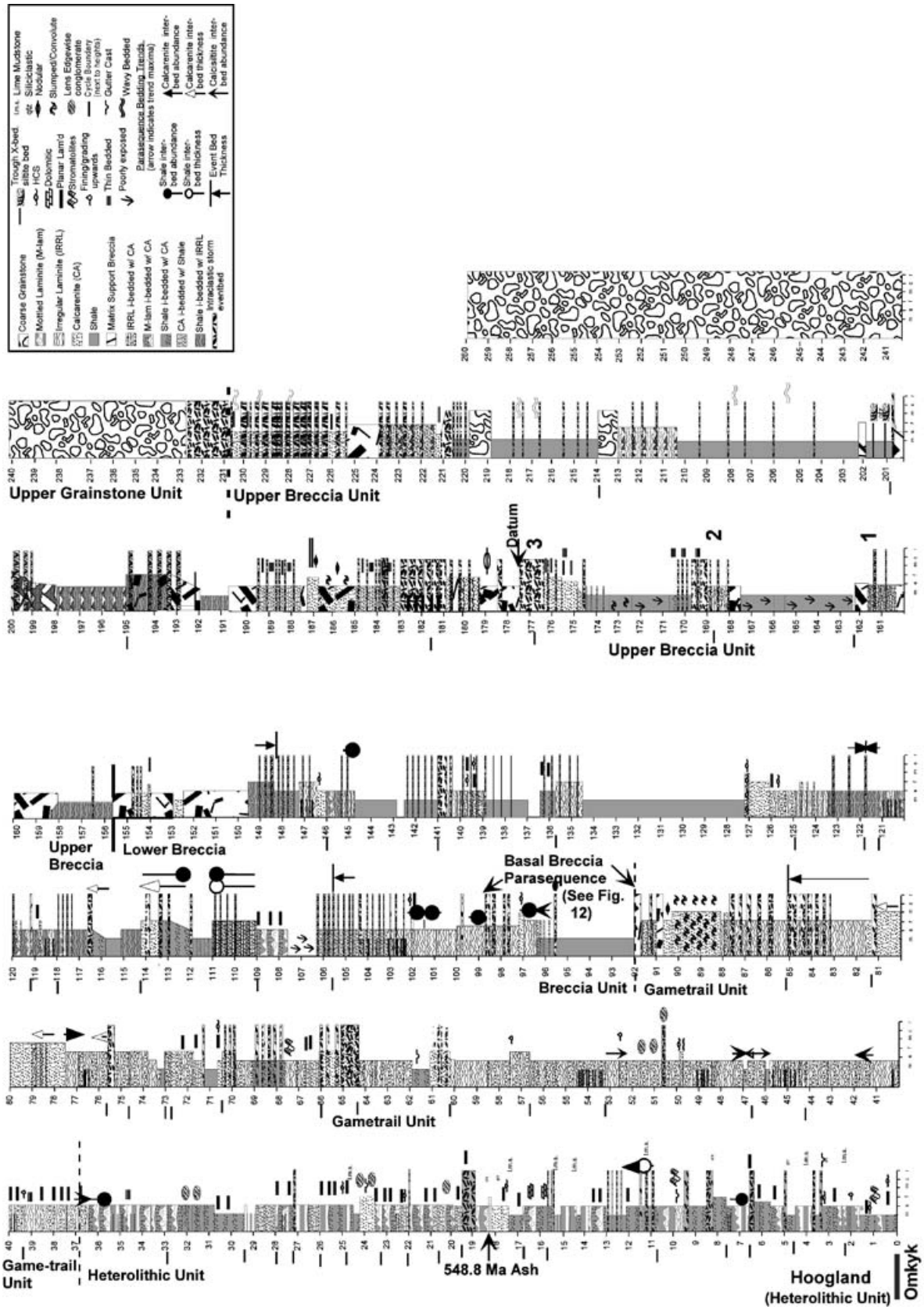

Figure 9. Reference section for Hoogland Member, measured near centre of field area (location on Fig. 2). This section is found downdip of the pinchout of the Lower Grainstone unit (see Fig. 8) but contains all other units. The prominent shale interval at the base of the Breccia unit represents the first significant incursion of shale onto the Hoogland platform and represents a significant change in parasequence construction reflected in overlying parasequences. Parasequences at this level and above grade upward from shaly bases into caps of storm-deposited carbonates; compare vertical facies succession with laterally adjacent facies in platform facies model (Fig. 3) and regional cross-section (Fig. 8). Also note larger-scale coarsening-upward sequence from 0–92 m.

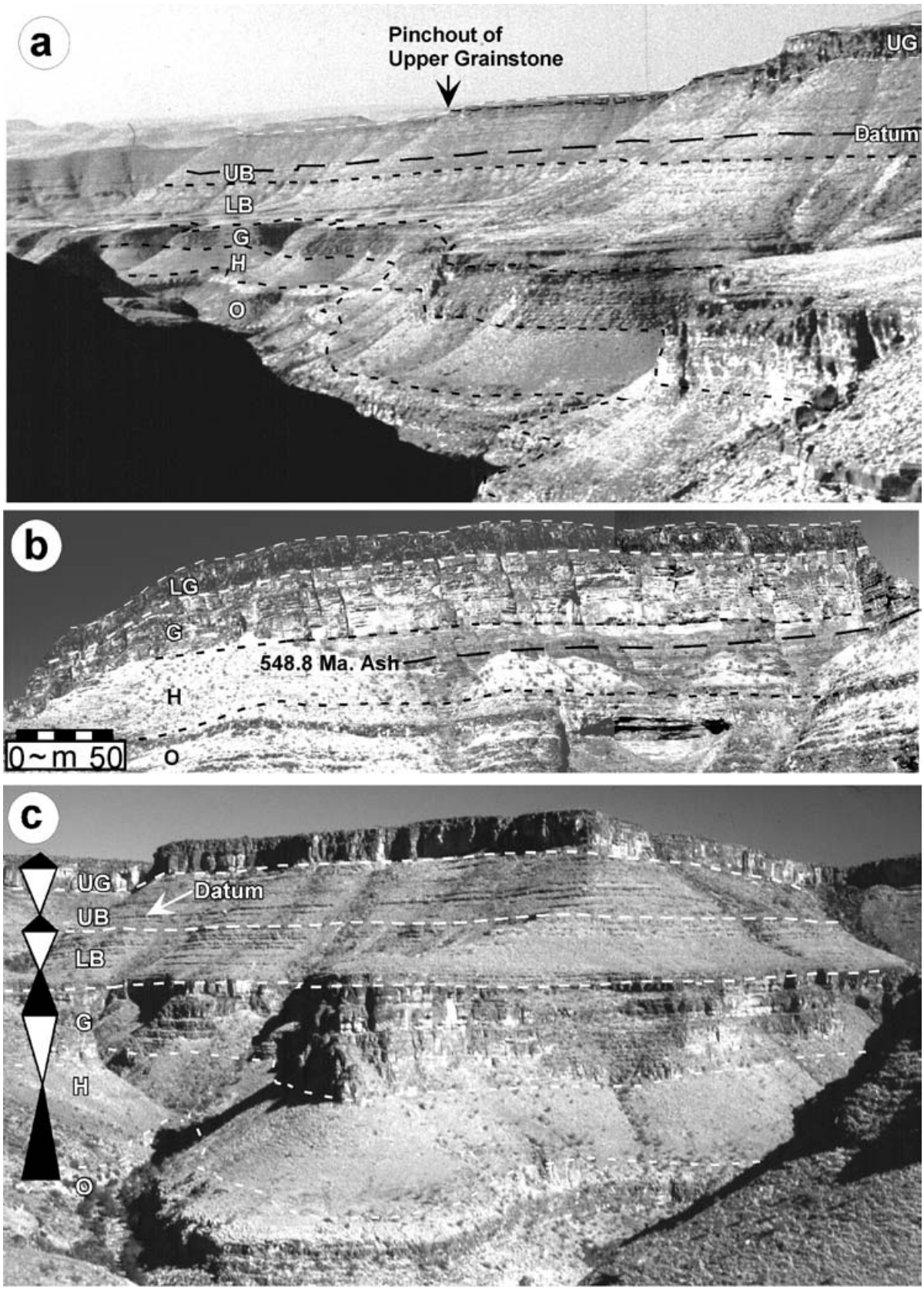

Figure 10. For legend see next page.

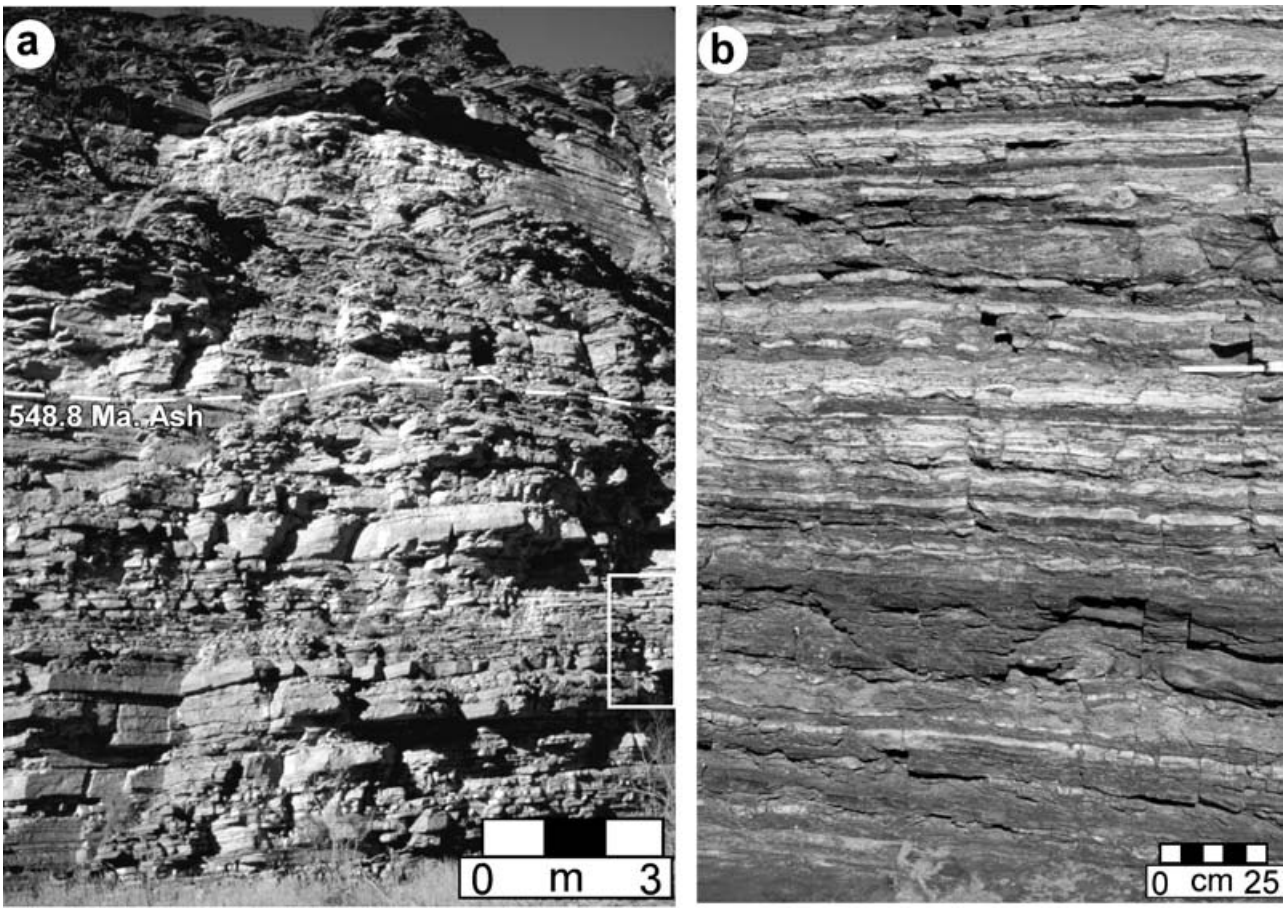

Figure 11. (a) Heterolithic unit showing fine to medium interbedding of heterolithic facies. Box represents relative size of enlargement in (b). (b) Close-up of heterolithic facies showing shales thinly interbedded with fine-grained calcisiltites and lime mudstones.

over 10 km, the highest continuity observed within the Hoogland Member.

The transition upward into the Gametrail unit marks a shift to progradational parasequence stacking and steeper lateral facies gradients (Figs 8, 9, 10b). This transition is expressed by: (1) an upward increase in the thickness and proportion of storm-deposited intraclastic beds including edgewise conglomerates; (2) replacement of mottled laminites by irregular laminites; (3) an increase in coarser-grained, quasi-planar-laminated and hummocky cross-stratified calcarenite; (4) increase in the degree of scouring; and (5) production of smoother stromatolites with greater elongation in the irregular laminite facies.

4.b. Gametrail unit

The Gametrail unit consists dominantly of parasequences containing irregular laminites interbedded with intraclastic conglomerate and planar-laminated to hummocky cross-laminated calcarenites, representing shallower, higher-energy conditions than in the underlying Heterolithic unit (Fig. 9). Lateral facies transitions occur over shorter distances than in the

Figure 10. Key photopans (see Fig. 2 for photo locations) (a) Outcrop stratigraphy of Hoogland Member. Note recessive Heterolithic unit (H) overlying Omkyk Member (O), parallel parasequences of Gametrail unit (G), shale-based, carbonate-capped parasequences of Breccia unit (LB and UB) and pinchout of Upper Grainstone unit (UG) further downdip than the Lower Grainstone unit (absent at this location). Datum is top of parasequence used in regional cross-section (Fig. 8) and traced in Figure 15. Height from base of valley to top of plateau is about 250 m. (b) Updip outcrop of the lower Hoogland Member illustrating shoaling from shaly, thinner-bedded Heterolithic unit into the carbonate-dominated Gametrail and Lower Grainstone units. Note thickness and massiveness of Lower Grainstone unit and compare sequence-scale shoaling here with parasequence-scale shoaling shown in Figure 14. (c) Outcrop photograph demonstrating presence of Upper Grainstone unit in positions downdip of the pinchout of the Lower Grainstone unit. The shale wedges at the bases of the Breccia unit's parasequences are interpreted to have infilled available downdip accommodation, allowing for the increased basinward progradation of coarse-grainstone facies over positions of underfilled accommodation. Also note the dolomitized reef in the uppermost Omkyk Member (light colour just above valley base), the recessiveness of the shale-rich Heterolithic unit, and the small, metre-scale, carbonate-dominated parasequences of the Gametrail unit. Height from base of valley to top of plateau is about 250 metres.

underlying Heterolithic unit (Fig. 8). These transitions involve downdip replacement of hummocky cross-stratified calcarenites, irregular laminites, and elongate stromatolites, all deposited by strong traction currents in updip ramp positions, by more thinly laminated irregular laminites and lime mudstones, both deposited through settling of suspended muds.

Parasequences of the Gametrail unit are 2–4 m thick and consist of thickening-upward, amalgamated beds of irregular laminites interbedded with an upward-increasing proportion of progressively thicker intraclast conglomerate beds (Fig. 9). Most of the Gametrail unit represents an early highstand systems tract (HST); most of the lower to middle portions of the Gametrail unit display a dominantly aggradational parasequence stacking pattern, with only a small component of seaward progradation that increases towards the top of the unit (Fig. 8).

Compared to the underlying Heterolithic unit, facies changes occur over a shorter lateral distance, implying steeper depositional gradients. This is interpreted to result from the shoaling and increased updip production of carbonate during highstand conditions that would act to produce a steeper platform slope due to higher updip carbonate sedimentation rates. Because of these marginally greater slopes, the physical processes involved in sediment formation and distribution would have been displaced, resulting in the observed foreshortening of facies belts upwards from the Heterolithic unit into the Gametrail unit.

4.c. Lower Grainstone unit

The Lower Grainstone unit is found only in updip positions overlying the Gametrail unit and represents the first significant occurrence of coarse-grained grainstones within the Hoogland Member (Figs 8, 10b). It consists of up to 25 m of cliff-forming, coarse, intraclastic, oolitic and composite-grain grainstone (Fig. 4a–c). Trough cross-bedding dominates in updip positions (Fig. 4a), but is replaced by hummocky cross-stratification in downdip positions. At its downdip limit, much of the Lower Grainstone unit can be traced into a single parasequence at the base of the overlying Breccia unit (Fig. 12), indicating significant partitioning of the volume of coarse-grained sediments. As a result, clinoform surfaces with dips up to 15° formed, and individual downdip-thinning tongues of grainstone can be traced to their pinchout. However, parasequences are not well expressed within the Lower Grainstone unit, except at its downdip limit where grainstones pass laterally into finer-grained sediments (Fig. 13).

The stratigraphic juxtaposition of the Lower Grainstone unit atop the Gametrail unit suggests emplacement as a late highstand, or lowstand systems tract (LST), and clinoform stacking patterns are observed to switch from forestepping to backstepping within the Lower Grainstone unit. The stratigraphic interval represented by the upper Gametrail unit through lower Breccia unit preserves the transition from HST to TST deposition without having experienced significant amounts of either erosion or bypass during accommodation minima. This is interpreted to reflect the relatively high tectonic subsidence rates expected for this foreland basin setting (cf. Read, 1980; Dorobek, 1995).

4.d. Breccia unit

The Breccia unit is a downdip-thickening wedge of shale-based parasequences that records the further encroachment of shales derived from the tectonically active, northern side of the foreland basin onto the Hoogland carbonate platform deposited along the southern, cratonic side of the foreland basin (Fig. 8). The Breccia unit varies in thickness from less than 90 m updip to over 250 m downdip. The Breccia unit overlies the Lower Grainstone unit in updip positions and rests directly on top of the Gametrail unit downdip of the Lower Grainstone pinchout (Figs 8, 10a, 10c, 12). It can be subdivided into lower and upper sub-units separated by a prominent marine flooding surface.

Parasequences are well developed within the Breccia unit and commonly possess a downdip-thickening basal wedge of shale that shallows upwards into downdip-thinning beds of irregular laminite and intraclastic conglomerate (Fig. 12). Updip, parasequences contain a carbonate-dominated assemblage of irregular laminites and thinly laminated calcisiltites that commonly are brecciated. These storm-disrupted intervals are capped by and pass downdip into individual 'tempestites' (Aigner, 1982; Myrow & Southard, 1996) consisting of an intraclastic conglomeratic base that grades upwards into a planar-laminated/hummocky cross-stratified to current- and wave-rippled cap (Fig. 14). Parasequences of the Breccia unit have well-defined flooding surfaces although their symmetry is variable; in some cases parasequence flooding is gradual and preserved as a thinning-upward succession of event beds, while others are more asymmetric, with caps of 5–20 cm thick tempestites that are abruptly overlain by pure shales (Fig. 9).

The base of the Breccia unit is placed within the backstepping TST near the Gametrail/Lower Grainstone–Breccia unit transition. Long-term accommodation increased upwards until the maximum flooding interval, located approximately four to seven parasequences above the basal parasequence of the Breccia unit. Above the maximum flooding interval the lower Breccia unit shows a forward-stepping parasequence pattern defined by lateral shifts in the spatial positions of both the capping irregular laminites and the locus of most intense syn-depositional brecciation. This forestepping pattern is terminated by a discrete flooding surface which marks the boundary that separates the lower Breccia unit from the upper Breccia unit and

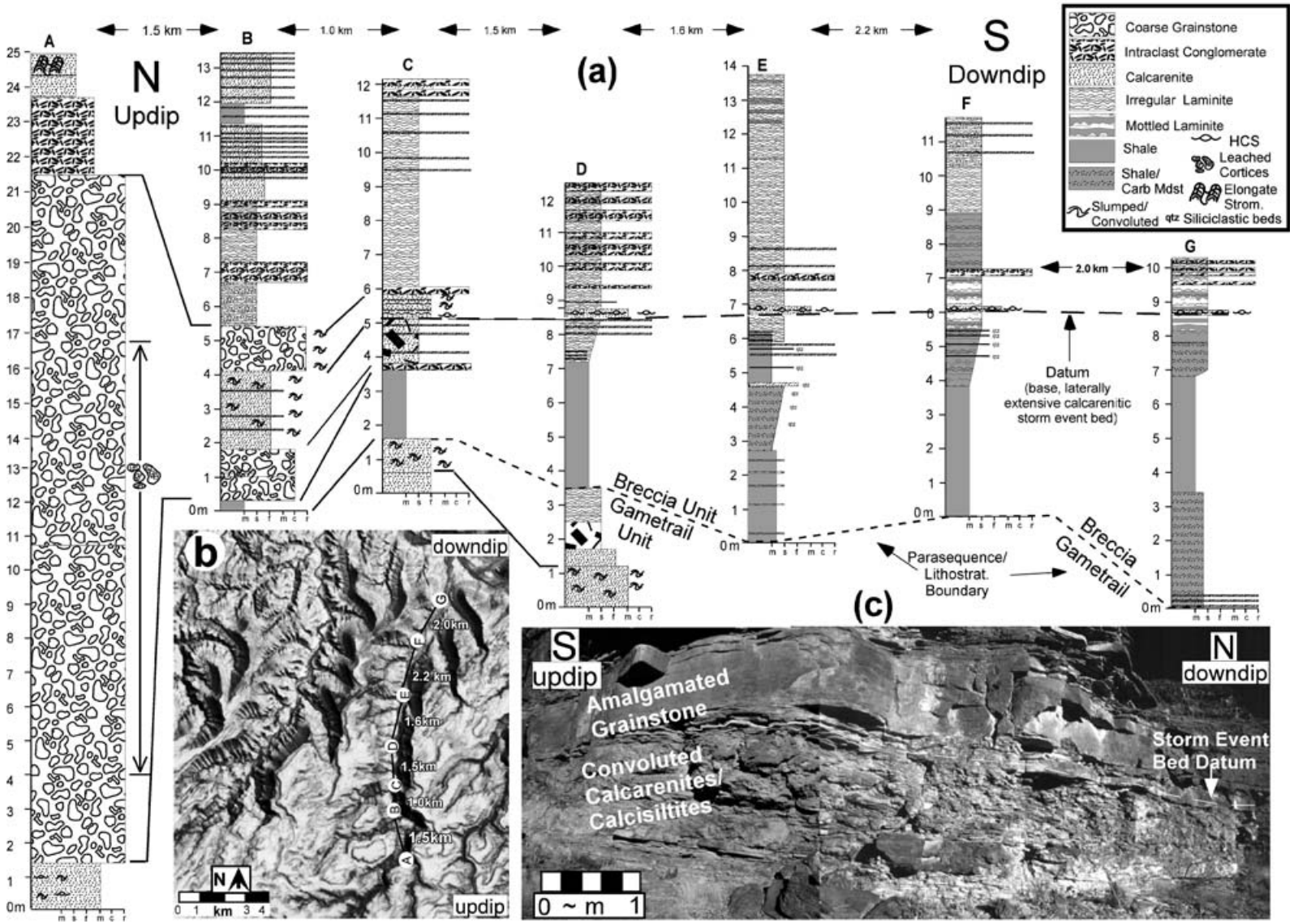

Figure 12. Dip-parallel transect of the prominent parasequence at the base of the Breccia unit. The stratigraphic interval immediately adjacent to the prominent storm bed used as the datum provides a snapshot of the lateral equivalency and extents of facies along a well-constrained and easily mapped chronostratigraphic horizon. Note downdip thickening of shale at base of parasequence and compare overall facies stacking with facies model in Figure 3. (b) Section localities in (a). (c) Outcrop photograph of coarse-grained facies immediately adjacent to storm event bed between sections B and C.

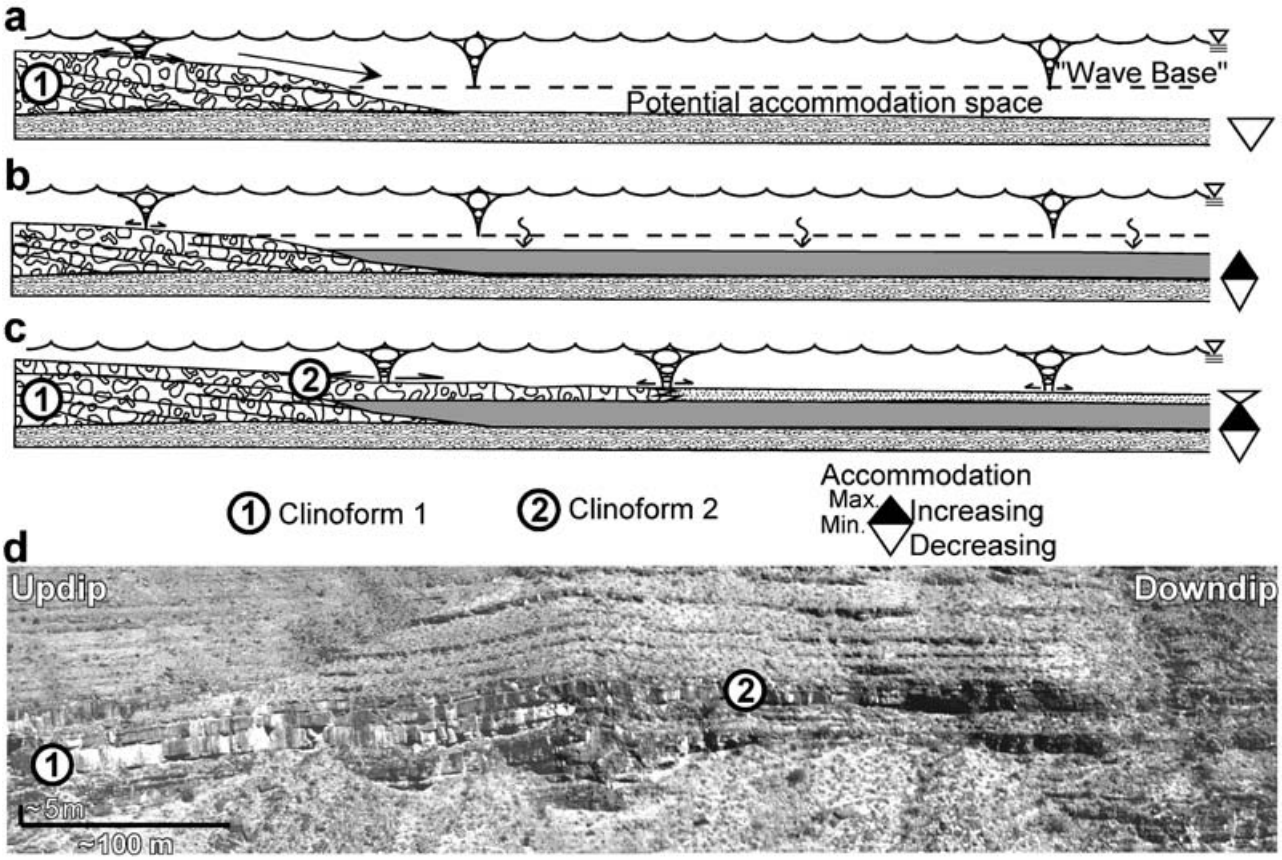

Figure 13. Pinchout of Lower Grainstone unit; see Figure 2 for location of photopan. (a) Transport and deposition of coarse-grained carbonate sediments (clinoform 1) downdip into positions of available accommodation below wave base. (b) Deposition of shale from suspension, sourced from a downdip direction, infills available downdip accommodation and decreases ramp slope. (c) Carbonate sedimentation resumes on a less steep platform transporting sediments (clinoform 2) further downdip. (d) Outcrop photograph of pinchout; note how lower, thicker clinoform (1) thins and pinches out further updip than the overlying thinner, yet more laterally extensive, clinoform (2).

results in a significant landward stepping of brecciated layers.

A backstepping pattern is displayed in the three successive parasequences above the lower–upper Breccia unit contact (Fig. 15). The third parasequence within this set is distinguished by its basal interval of thick, pure shale that extends the furthest updip of any shale in the Hoogland Member. Remarkably, however, the 2–5 m carbonate unit at the top of this terminal TST parasequence extends the furthest downdip of any carbonate interval within the Hoogland Member. Above this parasequence the Breccia unit foresteps as a HST through the middle of the Upper Grainstone unit.

4.e. Upper Grainstone unit

The Upper Grainstone unit comprises a downdip-thinning wedge of cliff-forming coarse grainstone facies. In updip positions, grainstone beds are entirely amalgamated, forming a composite stratigraphic thickness of up to 30-40 m (Fig. 10c). Amalgamation prevents delineation of parasequences in updip positions; however, the lateral transition of grainstones into shales in a downdip direction results in the development of metre-scale shale–grainstone couplets at intermediate palaeogeographic positions (Fig. 13). Grainstones within these couplets display a systematic change from updip and trough cross-bedded to downdip and hummocky cross-stratified with shaly partings.

The majority of the thickness of the Upper Grainstone forms a highstand systems tract of a depositional sequence that has its base at the contact between the lower and upper Breccia unit (Figs 9, 15). A sequence boundary occurs near the top of the Upper Grainstone which separates thicker, more massive, dominantly trough cross-stratified beds below from overlying hummocky cross-stratified thinner bedded grainstones with shaly partings. The surface lacks evidence for subaerial exposure but nonetheless represents a change from highstand to transgressive deposition. A flooding surface caps the backstepping interval of grainstones and results in the juxtaposition of pure shale on top of the last grainstone deposits of the Hoogland Member.

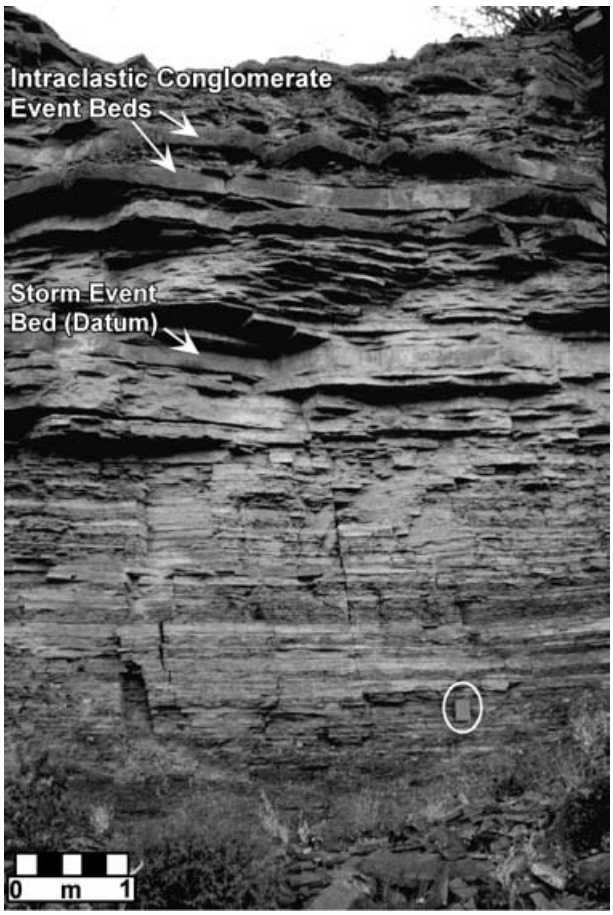

Figure 14. Basal Breccia unit parasequence near section E in Figure 12. Note upward increase in bedding thickness, decrease in proportion of shale, and attendant upward increase in carbonate sediment. Shoaling interpretation is based on the upward decrease in proportion of shale, in the thickening and coarsening of storm-deposited intraclastic conglomerate carbonate beds and by comparison of vertical stacking patterns with known chronostratigraphically constrained lateral facies equivalents. Fieldbook (circled) is 19 cm tall.

5. Discussion

The significant problem involved in the morphogenesis of the Hoogland ramp is how processes at the scale of individual beds interact, over space and time, with other processes that occur over longer times scales and potentially greater spatial scales, to build and maintain the ramp profile. This interaction is reflected in the manner in which beds build parasequences, which in turn build sequences, and eventually the platform as a whole. Models that describe the stratigraphic evolution of carbonate platforms must simulate the morphodynamic evolution of the depositional system, which reflects the interaction of important erosional as well as depositional processes.

The modelling approach which is taken will depend on what the compelling questions are, and also on what degree of physical approximation of those processes is acceptable when searching for mechanistic explanations. As in the case of terrestrial landscapes (cf. Dietrich *et al*. 2003), the morphodynamic evolution of carbonate systems should be directed at interpreting and predicting seascape form and evolution in some particular tectonic and climatic setting. For carbonate platforms, morphology is impressed in the rock record by facies distributions and stratal geometry. Whether terrestrial or marine, it is important to develop and test geomorphic transport laws, which are assumed to operate over some geomorphic temporal and spatial scale that integrates the effects of inherently stochastic and spatially variable processes. Several recent studies attempt to do this (e.g. Flemings & Grotzinger, 1996; Wilkinson *et al*. 1999; Drummond & Dugan, 1999; Burgess & Wright, 2003), but in each case the predicted seascapes (or resulting stratal geometries) are not compared closely with real ones. Instead, emphasis has been placed on the behaviour and form of hypothetical systems, using specific initial conditions, and boundary conditions and transport laws, to yield insight into the controls on real platform morphological evolution with predictions of facies distributions and stratal geometries.

Nevertheless, these studies provide valuable guidance and motivation for the analysis of scale-dependent processes that control carbonate platform development. In order to help stimulate the next generation of comparative studies, key processes involved in platform development should be evaluated and characterized through field observations which have been motivated by both physics-based (e.g. Flemings & Grotzinger, 1996) and rules-based (e.g. Drummond & Dugan, 1999; Burgess, Wright & Emery, 2001) process models.

5.a. Bed-scale effects on morphology

Processes acting at the bed scale can be considered a competition between three elements (Grotzinger & Knoll, 1999): (1) upward growth represented by relief-producing (sea-bottom surface-roughening) growth of biologically or inorganically precipitated material; (2) upward-directed accretion through deposition of suspended sediment; and (3) smoothing of sea-bottom relief through lateral transport of sediment from local sea-bottom highs to lows (Figs 6, 16). The wave-dominated environment during Hoogland time would have favoured the latter factor. Any high points formed through *in situ* growth would be subjected to relatively high basal shear stresses, which would tend to sweep sediments into adjacent lows. At a larger scale, sediment transport across the ramp under these wave-dominated conditions exhibits a net export of sediments from shallower updip areas and into downdip positions of greater available accommodation. These downdip areas are below wave base where the threshold for sediment transport is not exceeded during any storm of a given magnitude.

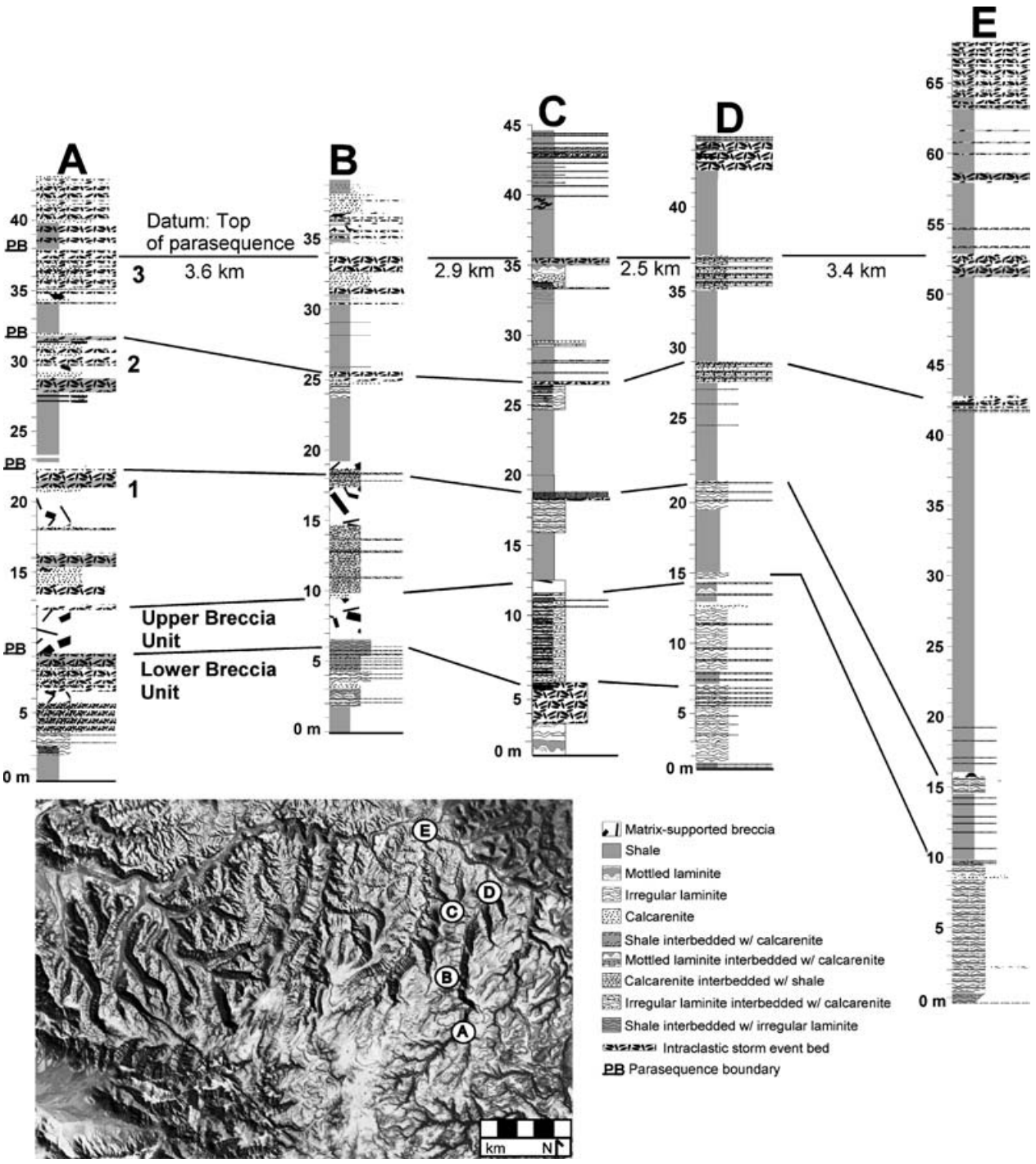

Figure 15. Dip-parallel transect through Lower–Upper Breccia unit contact. Thickening at base of parasequence two is observed in all dip-parallel cross-sections and demonstrates how greater amounts of downdip tectonic- and compaction-related subsidence were infilled by southward platform-tapering wedges of shale. Vertical scale in metres.

At the smallest scale that matters, biological (in this case, microbial) processes are fundamentally important to the morphological evolution of the Hoogland ramp (Figs 6, 16). Loose sediment deposited on the upper surface of microbial mats is tethered in place by the upward propagation of cyanobacterial sheaths through the sediment layer (Gebelein, 1974). It is readily apparent that the microbiota must physically compete with the influx of sedimentary detritus in order to populate the depositional interface at densities sufficient to maintain a coherent mat. Under conditions of relatively small sediment influx, all constituents of the mat community are capable of rising through a given sediment layer (Des Marais, 1995). Primary producers are displaced first, followed by an assemblage of consumers, degraders and anaerobic photobacteria. If

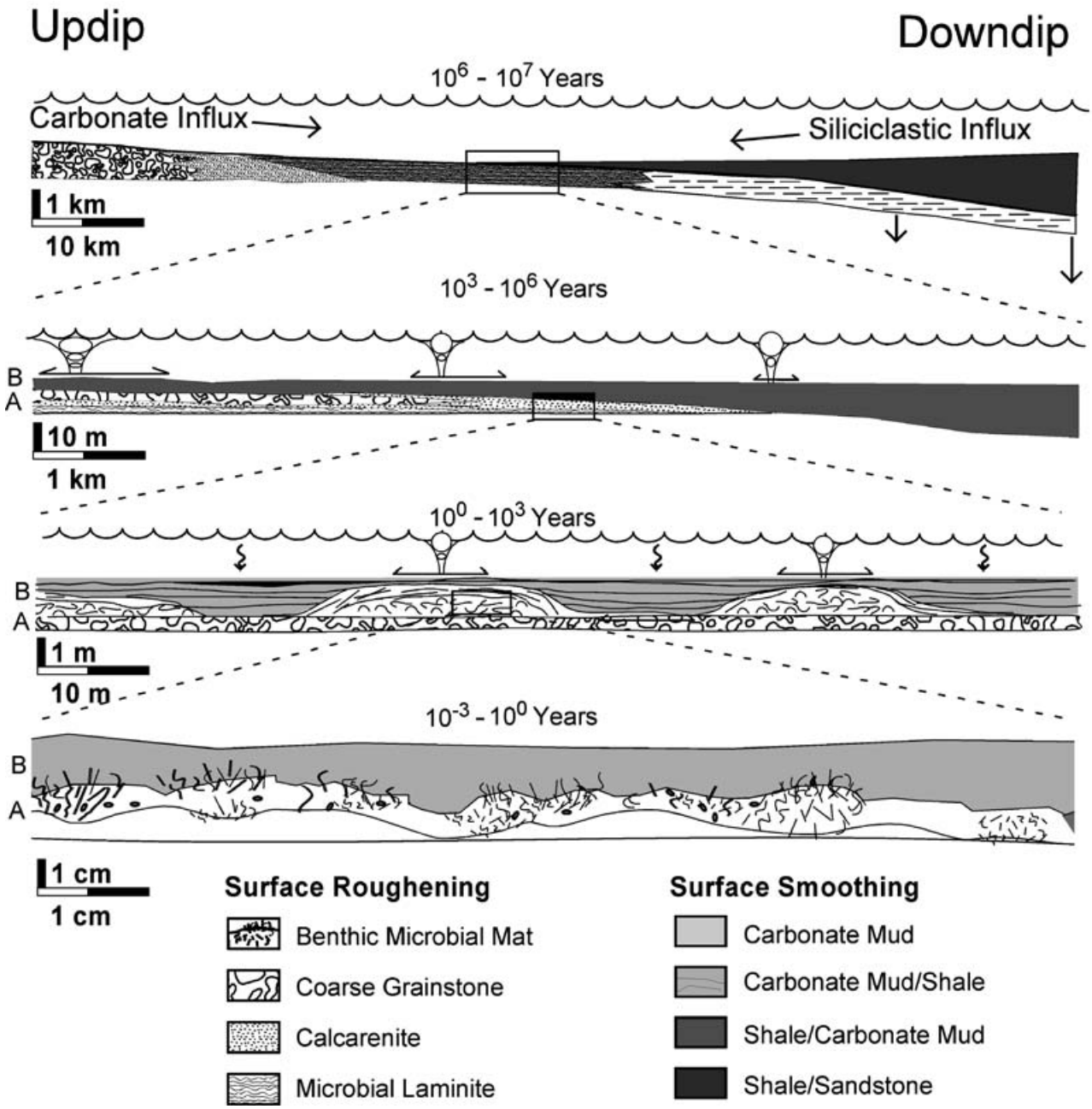

Figure 16. Summary of morphodynamic processes that affect Hoogland ramp development. The processes occur at a broad range of spatial and temporal scale. Note that ramp flatness is obtained as a result of the competition between processes that roughen the sea-floor and those that smooth it. At the shortest temporal and spatial scales, local processes such as growth of microbial mats and reefs are the principal agents of roughening, whereas at greater spatial and temporal scales, roughening is dominated by spatially dependent variations in the volume flux of sediments representing different facies tracts. At the shortest spatial and temporal scales, smoothing occurs as sediments transported across the platform during storms and fair-weather processes (e.g. whitings) are redistributed to fill the nooks and crannies created by mats and reefs. At greater spatial and temporal scales, smoothing is enhanced by the flux of shales derived from the orogenically active margin of the foreland basin, to fill, in a reciprocal manner, the accommodation created by differential carbonate accumulation.

a relatively higher sedimentation rate is sustained, then the proportion of filamentous cyanobacteria in mats increases relative to coccoid forms, because the gliding motility of filamentous forms provides a selective advantage (Des Marais, 1995). Logically, as the sedimentation rate increases past some (currently unknown) critical value, the sediment-stabilizing effect should drop off dramatically because sediment accumulation simply outpaces the maximum possible microbial response. The key point is that in natural systems there will be specific response times and scales for both microbial and sedimentation processes and

the growth of stromatolites will clearly be sensitive to how these processes balance. The endmember products of these interactions are clear. In the absence of sedimentation, mats will decay and stromatolites will not be formed due to a lack of building material. On the other hand, stromatolites will not develop in the presence of critically high sediment fluxes because mat growth is not sustainable. When a favourable balance is achieved between these two fluxes, growth of stromatolites (Fig. 4f) and larger microbialite mounds (Fig. 16) can be sustained.

An evaluation of the temporal and spatial scaling of these processes is critical to the understanding of platform morphogenesis. Additional studies of modern and experimental depositional systems are essential to address this problem because of the importance in quantifying sediment fluxes and mat growth rates. For example, what is the minimum thickness of a layer of sediment that is required to blanket and extinguish growth of an existing mat, so that it must recolonize? Alternatively, how frequently do tolerably thin layers have to be deposited before their integrated effect similarly results in termination of mat growth? Are either of these effects dependent on sediment grain size? How do these effects scale as a function of mat community structure? Only after these processes are fully characterized will it become possible to understand the significance of morphology as recorded in the smallest-scale building blocks of carbonate platforms dominated by microbialites, such as the Hoogland platform.

At somewhat greater scales (those of buildups; Fig. 16), the initial Hoogland platform had the potential to develop significant constructional relief as seen in thrombolitic reefs developed at multiple horizons in the underlying grainstone-dominated Omkyk Member (Grotzinger, Watters & Knoll, 2000; Grotzinger, 2000). However, by Hoogland time, the increased siliciclastic influx from the unroofing Damara Orogen created conditions unfavourable for nucleation and reef growth (cf. Turner, James & Narbonne, 1997). In such an increasingly siliciclastic environment the number of topographic relief-developing structures is limited as the mobility of the sea-bottom increases and the potential for early cementation decreases. Such an unconsolidated sea-floor, subject to the planing action of storm waves, would tend to maintain a relatively flat surface. These 'restoring' forces (so named because they counteract the effects of relief-building forces), whose influence is preserved in the constituent tempestites of parasequences, create and maintain the flat sea-floor by operating at the bed scale (Figs 6, 16). The beds of the individual parasequences are the building blocks of the parasequences. In turn, these stack to form the Hoogland ramp. Consequently, since the forces operating at the parasequence scale also act to plane the bottom flat, there is little chance that any relief could have developed and propagated significantly between beds, and then between parasequences.

5.b. Parasequence-scale effects on morphology

One key observation that results from correlation of beds and parasequences is that the spatial limits of storm-deposited carbonate beds at the tops of parasequences are greater when deposited over an underlying downdip thickening wedge of shale (Figs 13, 15). This suggests that infilling of downdip topography by shales is important in maintaining a regionally extensive surface of low slope, and recalls the reciprocal sedimentation model of Meissner (1971). This infilling is particularly evident at two stratigraphic levels described below: (1) within individual clinoforms of the Lower Grainstone unit (Fig. 13), and (2) within three parasequences immediately above the lower–upper Breccia unit contact (Fig. 15).

In the first example, the Lower Grainstone unit thins rapidly downdip from > 30 m to zero in approximately 5 km in the downdip direction (Figs 8, 12). At this point, the Lower Grainstone unit interfingers with shales of the basal Breccia unit and individual clinoforms can be traced to their pinchout. Progradation of the Lower Grainstone clinoforms was aided by the infilling of accommodation by shales. Figure 12 shows that the first clinoform (initial parasequence) downlaps directly against the upper contact of the Gametrail unit, to a point that marks only limited progradation. This was followed by infilling of accommodation by shales, with the subsequent effect that the overlying carbonate bed was able to extend further downdip than the previous carbonate bed. Infilling in this manner would have elevated the sea-floor and thereby subjected a greater area to storm wave influence, which would have acted to disperse carbonate sediments further into the basin (Fig. 13).

The second example occurs within the set of three parasequences immediately above the flooding surface defining the lower–upper Breccia unit contact. In a fashion similar to the first example, this succession of parasequences (Fig. 15) displays downdip thickening due mostly to thickening of shales in their lower parts. Shales deposited at the base of the middle parasequence exhibit the greatest amount of downdip thickening, implying that a significant amount of downdip accommodation was filled by the time of deposition of the more laterally extensive carbonate facies of the upper parasequence. The regionally extensive upper parasequence also demonstrates that intraclastic and granular carbonate sediments extend over much less area than fine-grained carbonate sediments deposited from suspension and gravity currents.

The efficiency of carbonate sediment transport would have been enhanced in the storm-dominated environment of the Hoogland platform. Considering the range of storm-wave energies that affected the sea-floor during deposition of a parasequence-scale oscillation in relative sea-level, storm-produced currents would have acted to effectively transport sediment

downdip into positions located below wave base. Along a depositional profile this can be considered to be the position where the threshold for sediment transport under oscillatory to combined flow conditions is not exceeded (Komar & Miller, 1974). During a storm and associated swell, the sea-floor will experience a spectrum of shear stresses; the cumulative effect of these stresses, when applied iteratively over long time scales, would be to plane off the sea bottom to a nearly horizontal surface. This is one of the key processes by which short-term, bed-scale processes likely affected the long-term morphology of the Hoogland ramp.

Changes in ramp declivity brought about by increased updip production (increase in slope), or downdip infilling by shales (decrease in slope), would have affected the area of wave-generated sea-floor shear stresses. Due to the interaction of the exponentially depth-decreasing wave orbital diameter (Grant & Madsen, 1986) with the nearly linear profile of the sea-floor, steeper slopes would have experienced steeper gradients in the amounts of storm-transported sediment and thus were subject to proportionately smaller downdip sediment transport. Steeper ramp slopes would have resulted in shorter-length scales for individual tempestite beds because of the smaller area within the zone exceeding the threshold for oscillatory and combined flow sediment transport. For more gentle slopes, correspondingly larger areas of the sea-floor would have experienced suprathreshold (Komar & Miller, 1974) conditions, and more laterally extensive beds would have been deposited (Fig. 5). Reports of both modern (Gagan, Johnson & Carter, 1988) and ancient offshore-thinning storm beds (Aigner, 1982) corroborate this model for a downdip-decreasing amount of storm-deposited sediment.

5.c. Sequence- and platform-scale effects on morphology

The architecture of the entire upper Hoogland Member from the Breccia unit through Upper Grainstone unit exhibits sequence-scale versions of the parasequence-scale patterns described above in which shales infill downdip accommodation, allowing carbonates to prograde greater distances at parasequence tops. In a similar fashion, the Upper Grainstone prograded a greater distance downdip than the Lower Grainstone unit because accommodation between the two was infilled by the Breccia unit's parasequences which contain downdip-thickening wedges of shale (Figs 8, 15). The Lower Grainstone unit, in contrast, downlapped directly onto the carbonate-dominated parasequences of the Gametrail unit, and was more limited in extent, owing to the lack of accommodation-filling parasequence-scale shale wedges.

The influx of shales in the Hoogland Member was a key process which contributed directly to maintaining low platform gradients, and the development of a ramp rather than rimmed shelf (Fig. 16). These relationships described at the parasequence and sequence scale at first seem paradoxical, given the often inimical relation between clastic influx and carbonate productivity. One expects that carbonates should prograde less efficiently given the demonstrated influx of clastics, due to the sensitivity of carbonate-producing organisms (even microbes: Grotzinger & Knoll, 1999) to siliciclastic influx. The resolution of this paradox lies in the fact that episodes of carbonate sedimentation and episodes of siliciclastic sedimentation seem to be out of phase, and mutually exclusive for the most part, such as in the case of the classic reciprocal sedimentation model (Meissner, 1971). Instead, siliciclastic sediments provide a beneficial feedback to the carbonate ramp system by infilling the accommodation produced in downdip positions, thereby allowing storm wave energy to be dissipated over a greater area, which can enhance transport of sediments to depositional sites located in more downdip positions. This positive feedback is a further important control which helps maintain a gentle ramp profile (Fig. 16).

At the largest scale, the shift to siliciclastic deposition which terminated platform growth is interpreted to relate to increased siliciclastic sediment flux related to progressive unroofing of the hinterland, combined with possibly decreased tectonic subsidence. Siliciclastic sediment influx simply overwhelmed carbonate production. This cessation of carbonate production due to siliciclastic burial of the platform is directly analogous to other foreland basins, such as the Taconic foredeep (Read, 1980; Cisne, 1982; Bradley & Kusky, 1986; Joy, Mitchell & Adhya, 2000).

6. Summary

(1) The Hoogland platform is a well-developed ramp formed in a high-energy, mixed carbonate–clastic, foreland basin setting. Ramp facies include updip coarse grainstones which grade downdip into finer grainstones, and then into broad, spatially extensive tracts of microbial laminites and finely laminated mudstones deposited above and below storm wave base. Siliciclastic siltstones and shales were deposited further downdip. Platform growth was terminated through smothering by orogen-derived siliciclastic facies.

(2) At the bed scale, facies patterns were controlled by upward growth of microbial mats, fallout of suspended sediment, and lateral transport of sediment through high bed-shear stress created by strong storm-induced flows. At the parasequence and sequence scales, facies patterns consist of alternating carbonates and wedges of shale derived from opposite sides of the foreland basin. Sediment fluxes from these opposed source areas acted to affect the length scales of the carbonate caps to the parasequences.

(3) Filling in of downdip accommodation space by the shales stimulated a positive feedback which allowed loose carbonate sediments to be transported

more efficiently downdip, which further contributed to smoothing gradients through additional accommodation infilling. The high degree of sediment mobility limited reef growth, and therefore precluded development of a well-defined shelf-edge, which in turn prevented the Hoogland platform from evolving into a rimmed shelf.

(4) The gentle profile of the Hoogland ramp was maintained by several processes that occur across a range of temporal and spatial scales, but share in common the net result that balance is achieved between processes that build relief and processes which dampen it (Fig. 16). At the smallest scale, 'roughening' of the sea-floor through heterogeneous trapping and binding by microbial mats was balanced by smoothing of the sea-floor through accumulation of loose sediment to fill the millimetre- to centimetre-scale nooks and crannies within the upward propagating mat. At the next scale up, parasequence development involved roughening of the sea-floor through shoal growth and grainstone progradation, balanced by sea-floor smoothing through shale infilling of resulting downdip accommodation. At even larger (sequence/platform) scales, roughening of the sea-floor occurred through aggradation and progradation of thick carbonates, such as the Upper Grainstone unit, balanced by infilling of the foreland basin with orogen-derived siliciclastic sediments.

Acknowledgements. The Geological Survey of Namibia is gratefully acknowledged for providing a field vehicle and logistical support for many years of research in Namibia. Wolf Hegenberger, Charlie Hoffman and Roger Swart are thanked for help in providing an introduction to the geology of Namibia, and for providing helpful guidance and advice. Roger Swart and NAMCOR are thanked for providing the Landsat TM image in Figure 2. Special thanks go to Rob and Marianne Field and Roy Magson for access to their farms, Zebra River and Donkergange, and for their hospitality. Support for this research was provided by NSF grants EAR-9904298 and EAR-0001018. Nic Beukes and Roger Swart reviewed the manuscript and suggested helpful way to improve it.

References

AIGNER, T. A. 1982. Calcareous Tempestites: Storm Dominated Stratification in Upper Muschelkalk Limestones (Middle Triassic, ZW Germany). In *Cyclic and Event Stratification* (eds G. Einsele and A. Seilacher), pp. 180–98. New York: Springer-Verlag.

ARNOTT, R. W. 1993. Quasi-planar laminated sandstone beds of the Lower Cretaceous Bootlegger Member, north-central Montana: Evidence of combined-flow sedimentation. *Journal of Sedimentary Petrology* **63**, 488–94.

BRADLEY, D. C. & KUSKY, T. M. 1986. Geologic evidence for rate of plate convergence during the Taconic arc-continent collision. *Journal of Geology* **94**, 667–81.

BURGESS, P. M. 2001. Modeling carbonate sequence development without relative sea-level oscillations. *Geology* **29**, 1127–30.

BURGESS, P. M. & WRIGHT, V. P. 2003. Numerical forward modeling of carbonate platform dynamics: An evaluation of complexity and completeness in carbonate strata. *Journal of Sedimentary Research* **73**, 637–52.

BURGESS, P. M., WRIGHT, V. P. & EMERY, D. 2001. Numerical forward modeling of peritidal parasequence development: implications for outcrop interpretation. *Basin Research* **13**, 1–16.

BURNE, R. V. & MOORE, L. S. 1987. Microbialites: Organosedimentary Deposits of Benthic Microbial Communities. *Palaios* **2**, 241–54.

CHAFETZ, H. S. & BUCZYNSKI, C. 1992. Bacterially induced lithification of microbial mats. *Palaios* **7**, 277–93.

CISNE, J. L., KARIG, D. E., RABE, B. D. & HAY, B. J. 1982. Topography and tectonics of the Taconic outer trench slope as revealed through gradient analysis of fossil assemblages. *Lethaia* **15**, 229–46.

CLUKEY, E. C., KULHAWY, F. H., LIU, P. L. F. & TATE, G. B. 1985. The impact of wave loads and pore-water pressure generation on initiation of sediment transport. *GeoMarine Letters* **5**, 177–83.

DES MARAIS, D. J. 1995. The biogeochemistry of hypersaline microbial mats. In *Advances in Microbial Ecology* (ed. G. J. Jones), pp. 251–74. New York: Plenum Press.

DIETRICH, W. E., BELLUGI, D., SKLAR, L., STOCK, J. D., HEIMSATH, A. M. & ROERING, J. J. 2003. Geomorphic Transport Laws for Predicting Landscape Form and Dynamics. In *Prediction in Geomorphology* (eds P. Wilcock and R. Iverson), pp. 103–32. AGU Geophysical Monograph no. 135.

DOROBEK, S. L. 1995. Synorogenic carbonate platforms and reefs in foreland basins: Controls on stratigraphic evolution and platform/reef morphology. In *Stratigraphic Evolution of Foreland Basins* (eds S. L. Dorobek and G. M. Ross), pp. 127–48. SEPM Special Publication no. 52. Tulsa: Society of Economic Mineralogists and Paleontologists.

DRUMMOND, C. N. & DUGAN, P. J. 1999. Self-organizing models of shallow-water carbonate accumulation. *Journal of Sedimentary Research* **69**, 939–46.

FLEMINGS, P. B. & GROTZINGER, J. P. 1996. STRATA: Freeware for analyzing classic stratigraphic problems. *GSA Today* **6**, 1–7.

GAGAN, M. K., JOHNSON, D. P. & CARTER, R. M. 1988. The Cyclone Winifred storm bed, central Great Barrier Reef shelf, Australia. *Journal of Sedimentary Petrology* **58**, 845–56.

GEBELEIN, C. D. 1974. Biologic control of stromatolite microstructure: implications for Precambrian time stratigraphy. *American Journal of Science* **274**, 575–98.

GERMS, G. J. B. 1983. Implications of a sedimentary facies and depositional environmental analysis of the Nama Group in South West Africa/Namibia. In *The Damara Orogen* (ed. R. Miller), pp. 89–114. Capetown: Geological Society of South Africa.

GRANT, W. D. & MADSEN, O. S. 1986. The Continental Shelf Bottom Boundary Layer. *Annual Review of Fluid Mechanics* **18**, 265–305.

GROTZINGER, J. P. 2000. Facies and paleoenvironmental setting of thrombolite–stromatolite reefs, terminal Proterozoic Nama Group (ca. 550–543 Ma), Central and Southern Namibia. In *Communications of the Geological Society of Namibia no. 12* (ed. R. M. Miller), pp. 221–33. Windhoek: Ministry of Mines and Energy.

GROTZINGER, J. P., BOWRING, S. A., SAYLOR, B. Z. & KAUFMAN, A. J. 1995. Biostratigraphic and geochronologic constraints on early animal evolution. *Science* **270**, 598–604.

GROTZINGER, J. P. & KNOLL, A. H. 1999. Stromatolites in Precambrian carbonates: Evolutionary mileposts, or environmental dipsticks. *Annual Review of Earth and Planetary Science* **27**, 313–58.

GROTZINGER, J. P., WATTERS, W. A. & KNOLL, A. H. 2000. Calcified metazoans in thrombolite–stromatolite reefs of the terminal Proterozoic Nama Group, Namibia. *Paleobiology* **26**, 334–59.

HOWARD, A. D. 1997. Badland morphology and evolution: Interpretation using a simulation model. *Earth Surface Processes and Landforms* **22**, 211–27.

JOY, M. P., MITCHELL, C. E. & ADHYA, S. 2000. Evidence of a tectonically driven sequence succession in the Middle Ordovician Taconic Foredeep. *Geology* **28**, 727–30.

KOMAR, P. D. & MILLER, M. C. 1974. The threshold of sediment movement under oscillatory water waves. *Journal of Sedimentary Petrology* **43**, 1101–10.

MEISSNER, F. F. 1971. Depositional patterns in middle Permian strata of central western United States. *American Association of Petroleum Geologists Bulletin* **55**, 539.

MOUNT, J. F. & KIDDER, D. 1993. Combined flow origin of edgewise intraclast conglomerates: Sellick Hill Formation (Lower Cambrian), South Australia. *Sedimentology* **40**, 315–29.

MYROW, P. M. & SOUTHARD, J. B. 1996. Tempestite Deposition. *Journal of Sedimentary Research* **66**, 875–87.

PAOLA, C., MULLIN, J., ELLIS, C., MOHRIG, D. C., SWENSON, J. B., PARKER, G., HICKSON,T., HELLER, P. L., PRATSON, L., SYVITSKI, J., SHEETS, B. & STRONG, N. 2001. Experimental stratigraphy. *GSA Today* **11**, 4–9.

RANKEY, E. C. 2002. Spatial patterns of sediment accumulation on a Holocene carbonate tidal flat, Northwest Andros Island, Bahamas. *Journal of Sedimentary Research* **72**, 591–601.

READ, J. F. 1980. Carbonate ramp-to-basin transitions and foreland basin evolution, Middle Ordovician, Virginia Appalachians. *American Association of Petroleum Geologists Bulletin* **64**, 1575–1612.

SEGURET, M., MOUSSINE-POUCHKINE, A., GABAGLIA, G. R. & BOUCHETTE, F. 2001. Storm Deposits and storm-generated coarse carbonate breccias on a pelagic outer shelf (South-East Basin, France). *Sedimentology* **48**, 231–54.

SIRINGAN, F. P. & ANDERSON, J. B. 1994. Modern shoreface and inner-shelf storm deposits off the East Texas coast. *Journal of Sedimentary Research* **64**, 99–110.

SUHAYDA, J. N. 1977. Surface waves and bottom sedmiment response. *Marine Geotechnology* **2**, 135–46.

TURNER, E. C., JAMES, N. P. & NARBONNE, G. M. 1997. Growth dynamics of Neoproterozoic calcimicrobial reefs, Mackenzie Mountains, Northwest Canada. *Journal of Sedimentary Research* **67**, 437–50.

WILKINSON, B. H., DRUMMOND, C. N., DIEDRICH, N. W. & ROTHMAN, E. D. 1999. Poisson Processes of Carbonate Accumulations on Paleozoic and Holocene Platforms. *Journal of Sedimentary Research* **69**, 338–50.